PHOSPHATIDYLINOSITOL 3-KINASE INHIBITION POTENTIATES GLUCOCORTICOID RESPONSE IN B-CELL ACUTE LYMPHOBLASTIC LEUKEMIA†

Running head: PI3K isoform inhibition in B-ALL

Cecilia Evangelisti[1§], Alessandra Cappellini[2§], Mariana Oliveira[3], Rita Fragoso[3], João T. Barata[3], Alice Bertaina[4], Franco Locatelli[4], Carolina Simioni[5], Luca M. Neri[5], Francesca Chiarini[6], Annalisa Lonetti[1], Francesca Buontempo[1], Ester Orsini[1], Andrea Pession[7], Lucia Manzoli[1], Alberto Maria Martelli[1*] and Camilla Evangelisti[6*]

[1]Department of Biomedical and Neuromotor Sciences, University of Bologna, Bologna, Italy

[2]Department of Human Social and Health Sciences, University of Cassino, Cassino, Italy

[3]Instituto de Medicina Molecular, Faculdade de Medicina, Universidade de Lisboa, Lisbon, Portugal

[4]Department of Pediatric Hematology-Oncology, IRCCS, Bambino Gesù Children's Hospital, Rome, Italy

[5]Department of Morphology, Surgery and Experimental Medicine, University of Ferrara, Ferrara, Italy.

[6]Institute of Molecular Genetics, Rizzoli Orthopedic Institute, National Research Council, Bologna, Italy

[7]Department of Medical and Surgical Sciences, University of Bologna, Bologna, Italy

§ These authors contributed equally to this work

*Correspondence:

- Alberto Maria Martelli, via Irnerio 48, 40126 Bologna, Italy, Phone: + 39 051 2091580, Fax: + 39 051 2091695, e-mail: alberto.martelli@unibo.it

- Camilla Evangelisti, via di Barbiano 1/10, 40136 Bologna, Phone: +39 051 2091581, Fax: + 39 051 2091695, e-mail: camilla.evangelisti@gmail.com

Conflicts of interest: The authors declare no conflicts of interest with respect to the authorship and/or publication of this article.

Contract grant sponsor: Programma Strategico "Innovative approaches to the diagnosis and pharmacogenetic based therapies of primary hepatic tumours, peripheral B and T – cell lymphomas and lymphoblastic leukaemias", Programma di Ricerca Regione-Università 2010–2012: Area 1 "Ricerca Innovativa" PRUa1RI-2012-001 to A.P.

Contract grant sponsor: PIC/IC/83023/2007 from Fundação para a Ciência e a Tecnologia (FCT), Portugal to J.T.B.

Abstract

Despite remarkable progress in polychemotherapy protocols, pediatric B-cell acute lymphoblastic leukemia (B-ALL) remains fatal in around 20% of cases. Hence, novel targeted therapies are needed for patients with poor prognosis. Glucocorticoids (GCs) are drugs commonly administrated for B-ALL treatment. Activation of the phosphatidylinositol 3-kinase (PI3K)/Akt/mammalian target of rapamycin signaling pathway is frequently observed in B-ALL and contributes to GC-resistance. Here, we analyzed for the first time to our knowledge, the therapeutic potential of pan and isoform-selective PI3K p110 inhibitors, alone or combined with dexamethasone (DEX), in B-ALL leukemia cell lines and patient samples. We found that a pan PI3K p110 inhibitor displayed the most powerful cytotoxic effects in B-ALL cells, by inducing cell cycle arrest and apoptosis. Both a pan PI3K p110 inhibitor and a dual γ/δ PI3K p110 inhibitor sensitized B-ALL cells to DEX by restoring nuclear translocation of the GC receptor and counteracted stroma-induced DEX-resistance. Finally, gene expression analysis documented that, on one hand the combination consisting of a pan PI3K p110 inhibitor and DEX strengthened the DEX-induced up- or down-regulation of several genes involved in apoptosis, while on the other, it rescued the effects of genes that might be involved in GC-resistance. Overall, our findings strongly suggest that PI3K p110 inhibition could be a promising strategy for treating B-ALL patients by improving GC therapeutic effects and/or overcoming GC-resistance.

Keywords: ALL, PI3K inhibitors, targeted therapy, dexamethasone

Introduction

B-cell acute lymphoblastic leukemia (B-ALL) is the most common malignancy in children, accounting for 80% of pediatric ALL (Graux, 2011; Siegel et al., 2012). Thank to progress in polychemotherapy protocols, the majority of B-ALL pediatric patients achieve complete remission. However, the prognosis of relapsed and chemoresistant patients remains poor (Harned and Gaynon, 2008). Also, infants and young adults with B-ALL display a much worse prognosis (Guest and Stam, 2017; Harned and Gaynon, 2008). Therefore, the identification of novel targeted therapies to support conventional chemotherapy is urgently required to further improve the outcome of this disorder.

Phosphatidylinositol 3-kinase (PI3K)/Akt/mammalian target of rapamycin (mTOR) (PI3K/Akt/mTOR) signaling pathway is a highly conserved signal transduction axis involved in many cellular processes (Laplante and Sabatini, 2012). It is well established that aberrant activation of this cascade is associated with the pathogenesis of several types of hematologic malignancies (Polak and Buitenhuis, 2012), including B-ALL (Fuka et al., 2012; Tasian et al., 2014). Therefore, this pathway is an attractive target to efficiently treat B-ALL patients. In particular, PI3K isoforms are now regarded as key targets for the development of innovative therapeutic strategies (Miller et al., 2017). PI3K is a family of enzymes grouped into three classes (I-III) with distinct structures and functions. Class I PI3Ks comprise four heterodimers that phosphorylate phosphatidylinositol-4,5-bisphosphate (PtdIns 4,5P_2) to yield PtdIns 3,4,5-trisphosphate (PtdIns 3,4,5P_3). PtdIns 3,4,5P_3 in turn recruits a number of downstream proteins containing a pleckstrin homology domain, including Akt. Class I PI3Ks, consisting of a p110 catalytic (-α, -β, -γ, -δ) and a regulatory subunit, display different patterns of expression in mammalian tissues. p110α and p110β catalytic subunits are ubiquitously expressed, whereas p110γ and p110δ catalytic subunits are mainly expressed in leukocytes (Chantry et al., 1997). Class I PI3Ks are the most studied class of isozymes and sustain

not only carcinogenesis, but also several tumor-promoting aspects of the neoplastic microenvironment (Engelman et al., 2006; Hanahan and Weinberg, 2011).

Over the last few years, several pan and isoform-selective class I PI3K p110 inhibitors have been disclosed by pharmaceutical companies. They display favorable drug properties and suppress tumor growth in different preclinical models of cancer. Therefore, some of them have recently entered clinical trials, also for hematological malignancies (Fruman and Rommel, 2014). Glucocorticoids (GCs) represent one of the most effective agents used in chemotherapeutic protocols for B-ALL, due to their strong pro-apoptotic activity to leukemic cells. Early response to GCs is one of the major prognostic factors of B-ALL, while GC-resistance has been associated with a poor outcome (Inaba and Pui, 2010; Kaspers et al., 1998). Despite their clinical significance, the molecular mechanisms underlying GC activity and resistance in lymphoid malignancies remain unclear (Bhadri et al., 2012; Norman and Hearing, 2002). In this connection, it is known that interactions between B-ALL cells and bone marrow stromal cells (BMSCs) in the marrow microenvironment can support leukemic cell survival and resistance to several drugs, including GCs (Randhawa et al., 2016).

Therefore, strategies aimed to reverse GC-resistance may considerably improve the outcome of B-ALL patients. It was recently shown that inhibition of the PI3K/Akt/mTOR pathway could reverse GC-resistance in ALL cells, as either MK2206 (an Akt inhibitor) or rapamycin (an mTOR inhibitor) were identified as GC sensitizers (Piovan et al., 2013; Wei et al., 2006).

Moreover, also migration of leukemic cells towards BMSCs is a poor prognostic factor in B-ALL (Aries et al., 2014; Konoplev et al., 2011). Therefore, molecules targeting motility of leukemic cells are interesting candidates for drug development to optimize treatment of B-ALL patients.

With the above in mind, we used preclinical models of B-ALL to test the cytotoxic effects of both pan and isoform-selective PI3K p110 inhibitors. Moreover, using dexamethasone (DEX), a GC frequently used in B-ALL therapy, we investigated the ability of PI3K p110 inhibitors to improve the therapeutic efficacy of GCs and/or their capability to decrease GC-resistance.

Materials and Methods

Cell lines, primary samples, human bone marrow stromal cells, and reagents

B-ALL cell lines (KOPN8, REH, NALM6) were obtained from Deutsche Sammlung von Mikroorganismen und Zellkulturen GmbH (DSMZ, Braunschweig, Germany). It is worth remembering that KOPN8 and REH cells are representative of infant and pediatric B-ALL, respectively, while NALM6 cells are representative of young adult B-ALL. All cell lines were cultured in RPMI-1640 medium (Life Technologies Italia, Monza, Italy) supplemented with 10% fetal bovine serum (FBS, Life Technologies). Samples from B-ALL pediatric patients were obtained after written and informed consent from the parents. Experimental protocols were in accordance with the guidelines and the regulations of the 1975 Helsinki declaration. The samples analyzed have been obtained from patients enrolled in the Associazione Italiana Ematologia Oncologia Pediatrica 2002/01 clinical trial, which was approved by the institutional review board of the Sant'Orsola Hospital, Bologna, Italy. Samples were isolated using Ficoll-Paque (Amersham Biosciences, Little Chalfont, UK) and grown in RPMI 1640 supplemented with 20% FBS and insulin-transferrin-sodium selenite. Human BMSCc (hBMSCs) were purchased from Creative Bioarray (Shirley NY, USA) and cultured in MSCGM™ Mesenchymal Stem Cell Growth Medium (Lonza, Williamsport PA, USA).

The PI3K p110 inhibitors (ZSTK-474, AS-605240, CAL-101, IPI-145), the Akt inhibitor (MK2206) and DEX were from Selleck Chemicals (Houston, TX, USA). Antibodies to PI3K p110δ and to glucocorticoid receptor (GR) were from Santa Cruz Biotechnology (Heidelberg, Germany), whereas the Ser134 p-GR antibody was from Merck Millipore (Darmstadt, Germania). All other primary and secondary antibodies were from Cell Signaling Technology (Danvers, MA, USA).

To test the effects of PI3K p110 inhibitors, B-ALL cell lines were cultured for 24 hours in the presence of the vehicle [0.1 % dimethylsulfoxide (DMSO)] or increasing drug concentrations, and cell viability was determined using the MTT [3-(4,5-Dimethylthythiazol-2-yl)-2,5-

diphenyltetrazolium bromide] cell proliferation kit (Roche Diagnostic, Basel, Switzerland) (Huang et al., 2017; Poli et al., 2017). The combination effects and potential synergism were evaluated by quantitative analysis of dose-effect relationship, based on the Chou and Talalay method (Chou and Talalay, 1984). For each combination experiment, a combination index (CI) was calculated using the CalcuSyn software (Biosoft, Cambridge, UK). This method of analysis generally defines CI values of <0.3 as strongly synergistic, 0.3 to 0.9 as synergistic, 0.9 to 1.1 as additive, whereas values >1.1 are considered antagonistic.

Annexin V-FITC/propidium iodide (PI) staining and cell cycle analysis

Apoptosis and cell cycle analysis were performed as previously described (He et al., 2016; Shrestha et al., 2016). B-ALL cell lines were treated with the different compounds or the vehicle alone. Analyses were performed on a FC500 flow cytometer (Beckman Coulter, Miami, FL, USA) with the appropriate software (CXP, Beckman Coulter).

Western blotting analysis

Western blotting analysis was performed by standard methods, as previously described (Ramazzotti et al., 2016; Tang et al., 2016). Cells were lysed using M-PER Mammalian Protein Extraction Reagent supplemented with the Protease and Phosphatase Inhibitor Cocktail (Thermo Fisher Scientific Inc., Rockford, IL, USA). Fifty μg of protein was loaded for each lane, unless otherwise specified. An antibody to β-actin was used as a loading control.

PtdIns 3,4,5P_3 quantification by flow cytometry

B-ALL cell lines were treated with the PI3K p110 inhibitors for 2 hours, fixed in 4% paraformaldehyde for 15 minutes, permeabilized in 0.4% Triton X-100 for 10 minutes, washed in phosphate-buffered saline (PBS) with 1% bovine serum albumin (BSA) and incubated over night at 4° with a FITC-conjugated anti-PtdIns 3,4,5P_3 antibody (Echelon, Biosciences Inc., Salt Lake City,

UT, USA). Analyses were performed on a FC500 flow cytometer with the appropriate software (CXP).

Immunofluorescence microscopy

Cells were seeded on electrostatically charged glass slides using a Shandon Cytospin (Thermo Electron Corporation, Pittsburgh, PA, USA) at low acceleration and 200 rpm for 5 min. Slides were fixed in 4% paraformaldehyde at 37°C for 10 min and permeabilized with 0.15% Triton X-100 in PBS for 8 min. Slides were then blocked with PBS containing 5% BSA for 1 hour. Incubation with anti-GR antibody (1:100) was performed overnight at 4°C in blocking medium. Then, a FITC-conjugated anti-mouse IgG antibody (1:200) was used for 1 hour at room temperature. Slides were washed 3 times for 10 min at room temperature with PBS/Tween 20 and mounted with a 4',6-diamidino-2-phenylindole (DAPI) anti-fade reagent in glycerol (Molecular Probes, Eugene, OR, USA). Images were taken on a Zeiss Axio ImagerZ1 microscope, equipped with 60X/NA 1.4 optics and Apotome apparatus, coupled to a computer driven Zeiss AxioCam digital camera (MRm), using Zeiss Axio Vision 4.4 software (Carl Zeiss, Oberkochen, Germany). All images were taken at similar exposures within an experiment for each antibody and processed using Adobe Photoshop 7 (Adobe Systems, San Jose, CA, USA).

Subcellular Fractionation

Cells were collected, centrifuged and washed in PBS. Pellets were resuspended in 1 ml of 10 mM Tris-HCl pH 7.4, 2 mM $MgCl_2$ for 2 minutes. Then, 0.6% Triton X-100 was added and the cells were passed twice through a syringe fitted with a 22 ½ gauge needle. Next, $MgCl_2$ was added to a final concentration of 5 mM and the samples were centrifuged for 10 minutes at 800 rpm. Nuclear pellets were washed twice in 10 mM Tris-HCl pH 7.4, 5 mM $MgCl_2$, while the supernatant was transferred to a new vial and used as a cytoplasmic fraction.

Migration assay and co-culture of B-ALL cells

Migration assay of B-ALL cells was performed using 24-well plates with Transwell® culture inserts (diameter 6.5 mm, pore size 8 μm; Costar Corning, New York, NY, USA). 1×10^6 cells were suspended in 100 μl of medium and added to the upper chamber. Inserts were transferred to bottom wells containing 600 μl of medium with or without 150 ng/mL of CXCL-12 (Biodesign International, Saco, ME, USA). Drugs or solvent were added and incubated for 4 hours at 37°C in 5% humidified CO_2 atmosphere. Inserts were then removed and cells transmigrated into the lower chamber were recovered and counted using an inverted microscope. Results are shown as the fold change of the percentage of migration compared with the untreated condition.

For co-colture, hBMSC were grown in the lower chamber of Transwell® 6-well plates containing a 0.4 μm polyester membrane (Corning) at a density of 5,000 to 6,000 cells/cm^2 (Frolova et al., 2012). Then, NALM6 and REH cells (375,000) were added to the upper chamber and treated with the drugs or solvent at the indicated concentrations. After 48 hours, the viability of drug-treated hBMSCs, NALM6, and REH cells, grown either alone or co-cultured, was evaluated by MTT assays.

Gene expression analysis

Total RNA was isolated from untreated cells and cells treated for 8 hours using a RNeasy Mini Kit (QIAGEN, Valencia, CA, USA) according to the manufacturer's instructions. Total RNA was reverse-transcribed into cDNA using the iScriptTM Advanced cDNA Synthesis Kit (Bio-rad, Hercules, CA, USA). Gene expression of GC signaling markers was measured using the PrimePCRTM Assay for real-time (Bio-rad). For each sample, cDNA was mixed with 2x SsoAdvancedTM universal supermix (25 ng cDNA/reaction) containing SYBR Green (Bio-rad) and aliquoted in equal volumes to each well of the real-time PCR arrays. The quantitative PCR reaction was performed using a 7300 Real-Time PCR system (Applied Biosystems, Foster City, CA, USA).

Statistical analysis

Statistical analyses were performed using Student's *t* test or one-way ANOVA (Dunnett's test) at a significance level of $p<0.05$ (GraphPad Prism Software, La Jolla, CA, USA).

Results

PI3K p110 inhibitors display cytotoxic effects in B-ALL cell lines

We investigated the efficacy of PI3K p110 inhibitors in suppressing leukemic cell proliferation and survival in *in vitro* models of B-ALL. We first evaluated the expression of PI3K p110 isoforms in a panel of B-ALL cell lines. All PI3K p110 isozymes were expressed in B-ALL cell lines, although protein levels varied (Fig. 1A). Then, the phosphorylation status of Akt (Ser473 and Thr308) and PTEN (Ser380) was studied. It is well established that, when phosphorylated at Ser380 by CK2, PTEN is post-translationally inactivated with a consequent PI3K/Akt/mTOR pathway activation in B-ALL cells (Gomes et al., 2014). Accordingly, all cell lines displayed activated (phosphorylated) Akt with a concomitant PTEN phosphorylation at Ser380 (Fig. 1A).

Next, we evaluated the viability of B-cell lines upon treatment with the pan PI3K p110 inhibitor ZSTK-474. As both p110γ and p110δ are highly expressed in B-lymphocytes, we also evaluated the isoform-selective inhibitors AS-605240 [selective to PI3K p110γ, (Camps et al., 2005)] and CAL-101 [(selective to PI3K p110δ (Herman et al., 2010)], as well as the γ/δ dual inhibitor IPI-145 (Duvelisib$^{@}$) and the combination AS-605240+CAL-101. IPI-145 antagonizes intrinsic and extrinsic survival signals in chronic lymphocytic leukemia (CLL) cells with an overactive PI3K/Akt/mTOR pathway (Dong et al., 2014).

Cells were treated for 24 hours with increasing concentrations of the drugs and the effects of PI3K p110 inhibitors on cell viability were analyzed by MTT assay (Fig. 1B). The pan PI3K p110 inhibitor ZSTK-474 displayed marked cytotoxic effects on all B-ALL cell lines (IC_{50} between 0.1 to 4.9 μM), whereas isoform-selective inhibitors were less cytotoxic and showed differences among

different cell lines (Table 1). Thereafter, the combination of p110δ (CAL-101) and p110γ (AS-605240) inhibitors at a fixed ratio (1:1) was evaluated. Interestingly, dual p110 γ/δ inhibition (using either IPI-145 or CAL-101 along with AS-605240) displayed stronger cytotoxic effects, especially in REH cells, compared to isoform-selective inhibitors (Fig. 1B and Table 1). In general, REH cells were the most sensitive to all PI3K inhibitors, whereas KOPN8 and NALM6 were more resistant, except to ZSTK-474.

Based on these results, in most of the following experiments we mainly focused on the two PI3K p110 inhibitors that showed the most potent cytotoxic effects on B-ALL cells, i.e. ZSTK-474 and IPI-145.

ZSTK-474 affects cell cycle progression, induces apoptosis and decreases migration of B-ALL cell lines

To determine whether treatment of B-ALL cell lines with PI3K p110 inhibitors could affect cell cycle progression, cells were incubated for 24 hours with the drugs and the cell cycle was studied by means of flow cytometric analysis of PI-stained samples (Fig. 2A). Only ZSTK-474 induced a statistically significant G_0/G_1 block and a concomitant decrease in both S and G_2/M phases of the cell cycle in all the cell lines tested.

Then, apoptosis induction was investigated by cytofluorimetric (Fig. 2B-C) and western blotting (Fig. 2D) analyses. Cells treated with ZSTK-474 underwent apoptosis after 24 hours of treatment, as demonstrated by the increased number of Annexin-V^+/PI^- and Annexin-V^+/PI^+ cells which correspond to early and late apoptosis, respectively (Fig. 2B-C).

Caspase-dependent apoptosis was further examined in B-ALL cells by western blotting analysis. A marked cleavage of caspase 3 as well as poly ADP-ribose polymerase (PARP) was induced by all the drugs, with the exception of AS-605240, in REH cells after 24 hours of treatment (Fig. 2D). On the contrary, NALM6 and KOPN8 cell lines resulted less sensitive to apoptosis, as documented by fainter or absent bands corresponding to cleaved-caspase 3 and PARP.

It is well established that CXCL12/CXCR4 axis is involved in many physiological and pathological processes, including tumor progression, angiogenesis, metastasis and survival (Teicher and Fricker, 2010). CXCL12 is secreted by BMSCs and plays an important role in homing, migration and survival of both hematopoietic progenitor cells and leukemic cells (Burger and Peled, 2009), including B-ALL cells (Bradstock et al., 2000). Indeed, the G-protein-coupled transmembrane receptor CXCR4 is highly expressed in B-ALL, where it is involved in survival of leukemic cells (Bradstock et al., 2000). Moreover, high levels of CXCR4 are linked to poor patient outcome in B-ALL patients (Konoplev et al., 2011; van den Berk et al., 2014).

Therefore, we investigated whether PI3K inhibitors could affect migration of B-ALL cells. KOPN8, NALM6 and REH cells were treated with either ZSTK-474 or IPI-145 for 4 hours and migration toward CXCL12 was measured using Transwell$^{@}$ assays. Both PI3K inhibitors strongly reduced (approximately 80%) migration of REH cells compared to controls, whereas reduction of transmigration was observed to a lower extent in both NALM6 and KOPN8 cells (Fig. 2E).

PI3K p110 inhibitors down-modulate PI3K/Akt/mTOR signaling

To confirm that ZSTK-474 and IPI-145 inhibited PI3K activity at the concentrations we used, PtdIns 3,4,5P_3 levels were measured in B-ALL cells. Cells were treated with either drug and flow cytometric analysis was performed. ZSTK-474 and, to a lower extent, IPI-145 were both able to significantly reduce the percentage of PtdIns3,4,5P_3-positive in all the three cell lines (Fig. 3A). Therefore, we examined the effects of PI3K p110 inhibitors on PI3K/Akt/mTOR signaling pathway effectors through western blot analysis (Fig. 3B). After 4 hours of drug treatment, we observed that ZSTK-474 negatively affected PI3K downstream targets in all the cell lines analyzed, as indicated by a marked dephosphorylation of Akt (both at Ser473 and at Thr308) and S6 ribosomal protein (S6RP). Similar effects were obtained in NALM6 and REH cells treated with IPI-145 (Fig. 3B).

PI3K p110 inhibitors synergize with GCs

To further evaluate the clinical potential of PI3K inhibitors in B-ALL treatment, we investigated whether these drugs could synergize with DEX, a GC commonly used for the treatment of pediatric B-ALL patients. Firstly, cells were incubated for 24 hours with increasing concentrations of DEX and cell viability was measured via MTT assays. As shown in Figure 4A, DEX reduced viability of REH, NALM6 and, to a lower extent, KOPN8 cell lines.

Then, the existence of possible synergisms of PI3K inhibitors (ZSTK-474 and IPI-145) with DEX was analyzed (Fig. 4B). Cells were treated for 24 hours with one of the above-mentioned drugs, alone or combined to DEX at a fixed ratio (DEX:PI3K inhibitors, 1:50) and CIs were calculated. A strong synergism of DEX with IPI-145 and, less frequently, with ZSTK-474, was observed in the analyzed cell lines, including KOPN8 cells, the most resistant cells both to PI3K p110 inhibitors and to DEX (Table 2). Synergisms induced by the combination of DEX with AS-605240, CAL-101 and AS-605240 + CAL-101 were in general less strong or undetectable in all the three cell lines analyzed (Table 2).

We further tested the pro-apoptotic effects of combination treatments. Cells were stained with Annexin V-FITC/PI and flow cytometric analysis was performed. The combination of DEX with either ZSTK-474 or IPI-145 was more effective in inducing apoptosis in all B-ALL cell lines analyzed when compared to single drug treatment, thus confirming that PI3K p110 inhibitors sensitized B-ALL cells to GCs (Fig. 5A). Moreover, apoptosis induction was confirmed by caspase 3 and PARP cleavage in KOPN8, NALM6 and REH cells, as documented by western blotting analysis in samples treated with the drug combinations (Fig. 5B).

The Bcl-2 family proteins are critical in mediating GC-induced apoptosis and could be involved in GC resistance (Bachmann et al., 2005). In particular, it has been observed that reduction of pro-apoptotic Bim expression (Jiang et al., 2011) as well as increase of anti-apoptotic Mcl-1 levels (Holleman et al., 2004) are related to GC resistance in pediatric ALL. We, therefore, analyzed the effects of treatment with DEX, ZSTK-474 or IPI-145, alone or in combination, on Bim and Mcl-1

expression in KOPN8, NALM6 and REH cells. Western blotting analysis documented a decrease of Mcl-1 expression in response to DEX plus PI3K inhibitor treatment and a concomitant increase of Bim in all cell lines studied (Fig. 5C).

PI3K p110 inhibition counteracts stroma-induced DEX resistance

Since human hBMSCs are known to be responsible for DEX-resistance *in vitro* (Randhawa et al., 2016), we investigated whether PI3K p110 inhibitors could reverse DEX-resistance in NALM6 and REH cells co-cultured with hBMSCs in a Transwell$^{@}$ system.

At first, we demonstrated that DEX and PI3K inhibitors did not affect hBMSC viability, as documented by MTT assays (Fig. 6A). Secondly, we observed that either ZSTK-474 or IPI-145 were able to partially counteract the increase in both NALM6 and REH leukemic cell viability in response to DEX treatment caused by co-culturing with hBMSCs (Fig. 6B).

PI3K p110 inhibitors induce GR nuclear translocation

GC cytotoxicity is mediated by binding of GCs to their intracellular receptor, GR, which is a ligand-inducible transcription factor (Whitfield et al., 1999). Indeed, when DEX binds to GR, the receptor is activated and translocates to the nucleus, thus activating the transcription of target genes that induce cell cycle arrest and apoptosis (Inaba and Pui, 2010).

In order to determine whether resistance to DEX correlated with GR down-regulation, basal levels of GR protein were compared among B-ALL cell lines by western blotting analysis. However, GR was expressed at approximately equivalent levels in all cell lines (Fig. 7A). The phosphorylation status of GR was then investigated. It has been documented that GR phosphorylation at Ser134 plays an important role in the modulation of GC-driven apoptosis (Galliher-Beckley et al., 2011; Piovan et al., 2013). Indeed, when GR is phosphorylated at Ser134, a nuclear translocation impairment occurs and this interferes with the patterns of GC-induced genes. Of note, this mechanism is regulated by Akt in T-ALL cells (Piovan et al., 2013). In order to investigate whether

PI3K/Akt signaling was involved in Ser134 phosphorylation and in nuclear translocation also in B-ALL cells, KOPN8 and NALM6 cells were treated with DEX, IPI-145 or ZSTK-474, and western blotting analysis for Ser134 p-GR was carried out. PI3K inhibitor treatment caused a marked dephosphorylation of GR at Ser134 (Fig. 7B), whereas DEX alone did not. A similar inhibitory effect was caused by MK2206, an allosteric Akt inhibitor (Hirai et al., 2010), thus confirming the crucial role played by Akt in this phenomenon.

As the GC-induced apoptotic response depends on translocation of the receptor-ligand complex to the nucleus, GR nuclear translocation was investigated by immunofluorescence and western blotting analyses following a 4 hours treatment with DEX in less sensitive cell lines, namely NALM6 and KOPN8 cells. As shown in Figure 7C, GR was predominantly cytoplasmic in untreated and drug-treated (ZSTK-474 or IPI-145) samples, while DEX caused a partial re-localization of GR to the nucleus. On the contrary, the combination of DEX with either ZSTK-474 or IPI-145 caused a striking nuclear translocation of GR. Similar results regarding GR localization were obtained by western blotting analysis in NALM6 cells (Fig. 7D).

Gene expression analysis

To study in more depth the synergisms between PI3K inhibitors and GCs in B-ALL cells, the GC signaling pathway was analyzed in NALM6 cells using a quantitative real-time PCR array with 82 genes (Supplementary Table S1).

A 8 hour treatment with the drugs (DEX or ZSTK-474), either used alone or in combination, was chosen in order to identify genes that were modulated in early phases of GC activation (Jing et al., 2015). Only differentially expressed genes (fold-change ≥ 2) were considered (Fig. 8A-B).

Thirty-one genes, of which four were induced and 27 repressed, were modulated in ZSTK-474 + DEX versus CTR samples (Fig. 8A and Supplementary Table S2). De-regulation of transcripts involved in signal transduction (e.g. *PI3KR1*, *RGS2*, *SESN1*, *SPHK1* and *USP2*), nucleotide metabolism (e.g. *AMPD3*), glucose and fatty acid metabolism (e.g. *ASPH*, *GOT1* and *H6PD*),

cytokines and chemokines (e.g. *EDN1* and *TNF*), cell surface receptors (*PDGFRB* and *VLDLR*) as well as transcription factors (e.g. *ARID5B*, *FOSL2*, *TSC22D3* and *BCL6*) was observed. In particular, ZSTK-474 combined with DEX induced a remarkable up-regulation of *TSC22D3*, a gene that plays a pivotal role in the anti-inflammatory and immunosuppressive effects of glucocorticoids (Bruscoli et al., 2015) as well as a down-regulation of several genes associated with cellular proliferation and survival such as *BLC6*, *CREB3*, *EDN1*, *PIK3R1*, *SPHK1*, *STAT5B* and *USP2*. In order to gain further insight into the mechanisms that might influence the synergism between GCs and PI3K inhibitors, we also analyzed genes differentially expressed in ZSTK-474 + DEX versus DEX alone samples (Fig. 8B and Supplementary Table S3). ZSTK-474 rescued the effects of genes that might be involved in GC resistance given that their expression goes in an opposite direction to GC-cytotoxic effects. For instance, DEX alone increased the expression of genes involved in cell survival such as *AQP1*, *CTGF*, *DDIT4*, *FKBP5* and *IL10*, while the addition of ZSTK-474 counteracted this effect, restoring the balance toward a cell death fate. In particular, *DDIT4* blocks cell growth, proliferation and survival through negative regulation of mTOR (Sofer et al., 2005) and *FKBP5* functions as a tumor suppressor of PI3K/Akt/mTOR signaling when it is hyper-activated (Li et al., 2011). Finally, ZSTK-474 was able to counteract the increase in *AQP1* and *CTGF* mRNA, a water channel protein and a growth factor respectively, both involved in cell growth and migration (Chu et al., 2008; Papadopoulos et al., 2008).

PI3K p110 inhibitors and DEX display synergistic cytotoxic effects in B-ALL patient lymphoblasts

To better evaluate the efficacy of PI3K inhibitors combined with DEX as potential therapeutic agents, we analyzed four pediatric B-ALL patient samples, isolated from peripheral blood. The effects of PI3K p110 inhibitors were first evaluated by performing MTT assays (Fig. 9A). Cells were incubated with either single drugs (DEX, IPI-145, ZSTK-474) or their combinations at a fixed ratio (DEX:PI3K inhibitor ratio, 1:50). A marked reduction of cell viability was detected, thus

documenting that the combined treatments were effective also in primary samples. The strongest effects were observed with the ZSTK+DEX combination.

Then, we analyzed apoptosis induction following combined treatment using Annexin V-FITC/PI staining. Flow cytometric analysis showed that both drug combinations increased apoptosis when compared to single drug treatments (Fig. 9B). Finally, the effects on the PI3K/Akt/mTOR pathway were assessed by western blotting after 24 hours of treatment with ZSTK-474 or IPI-145, used either alone or combined with DEX in a representative patient sample (Fig. 9C). High levels of p-Akt, p-S6RP and p-4EBP1 were observed in untreated lymphoblasts which indicated a constitutive activation of the PI3K/Akt/mTOR signaling axis. Drug treatments caused a marked decrease in the levels the phosphoproteins, documenting an inhibition of this signaling pathway.

Discussion

Over the last 40 years, the survival rate for pediatric B-ALL has increased from 30% to 80% (Pui and Evans, 2006). Protocols used to treat B-ALL include GCs, vincristine and asparaginase, with or without anthracyclines. However, relapsing B-ALL pediatric patients persist and this remains a leading cause of childhood morbidity and mortality. This therapy failure is mostly due to GC-resistance that is widely recognized as a determinant of poor prognosis (Den Boer et al., 2003). GCs are cytotoxic not only to neoplastic lymphoid cells, but also to healthy lymphocytes, thereby increasing the risk of severe infections. Furthermore, other adverse effects of GC therapy include hyperglycemia, osteonecrosis, neuropsychological alterations and myopathy (Inaba and Pui, 2010). In light of this, it is urgent to develop novel therapeutic strategies against B-ALL cells aimed to further optimize therapeutic regimens and to overcome GC-resistance.

The PI3K/Akt/mTOR pathway is aberrantly activated in hematological malignancies, including T-ALL and B-ALL (Khwaja, 2010) and It has been demonstrated that up-regulation of this signaling network is associated with bad prognosis and GC-resistance, both in T-ALL and B-ALL (Morishita et al., 2012; Silva et al., 2008). For instance, it is known that Akt activation underlies GC-resistance

in T-ALL via a direct phosphorylation of GR at the Ser134 residue (Piovan et al., 2013) and PI3K p110 inhibitors sensitized resistant MLL-rearranged ALL cells to prednisolone (Spijkers-Hagelstein et al., 2014). Therefore, PI3K p110 inhibitors are regarded as innovative drugs for the treatment of these types of blood cancer.

While in T-ALL it has been investigated whether either pan or isoform-selective PI3K p110 inhibitors are more cytotoxic to leukemic cells (Lonetti et al., 2015; Stengel et al., 2013; Subramaniam et al., 2012), similar studies have not been performed at all in B-ALL.

Starting from these premises, the aim of this study was to investigate the therapeutic potential of PI3K p110 inhibitors, alone and in combination with DEX, using a panel of B-ALL cell lines and primary samples. We tested pan, isoform-selective (γ or δ) and dual γ/δ PI3K p110 inhibitors, and evaluated their cytotoxic effects. To the best of our knowledge this is the first time that the effects of these drugs were analyzed in B-ALL cells.

We showed that the strongest cytotoxic effects against B-ALL cells were displayed by ZSTK-474, a novel pan PI3K p110 inhibitor that has entered clinical trials in patients with advanced solid malignancies (NCT01682473 and NCT01280487). ZSTK-474 reduced cell viability in a concentration-dependent manner, as demonstrated by MTT assays. Flow cytometric and western blotting analyses documented that ZSTK-474 cytotoxic effects were associated with both cell cycle arrest and apoptosis induction. ZSTK-474 induced a dephosphorylation of downstream targets of PI3K, namely Akt and S6RP. A decrease in PtdIns 3,4,5P_3 levels following treatment with ZSTK-474 was also detected. White blood cells are enriched in PI3Kp110γ and δ catalytic isoforms (Chantry et al., 1997). Therefore, the use of either selective (γ or δ) or dual γ/δ PI3K p110 inhibitors is considered as an innovative, rationale-based therapeutic strategy for hematological malignancies. Indeed, the use of these inhibitors should reduce toxicity and adverse effects in patients when compared to pan PI3K p110 inhibitors. For instance, safety and efficacy of the dual γ/δ PI3K p110 inhibitor IPI-145 have been already documented, as this drug entered clinical trials for treating non-Hodgkin lymphoma (Curran and Smith, 2014) and CLL (Balakrishnan et al., 2015) patients.

However, both selective and dual PI3K p110 inhibitors showed weaker effects on B-ALL cell viability when compared with ZSTK-474. In our study, only IPI-145 displayed anti-leukemic effects when administrated alone, but not in all tested cell lines. In particular, only REH cells were sensitive to IPI-145, displaying an IC_{50} of 2.6 μM. No significant synergy between AS-605240 and CAL-101 was seen in B-ALL cells as far as Akt dephoshorylation was concerned. This suggests that PI3K p110δ is likely the most important isoform involved in Akt phosphorylation (but not in S6 ribosomal protein phosphorylation) in B-ALL cell lines. Nevertheless, the cytotoxic effects of either CAL-101 or IPI-145 were generally inferior to ZSTK-474, supporting the concept that also in B-ALL inhibition of all PI3K p110 catalytic subunit is required to attain the strongest cytotoxic effects. This is in agreement with the results previously reported by our group for T-ALL (Lonetti et al., 2015; Stengel et al., 2013).

Intriguingly, we observed that the REH cell line is sensitive to both pan and selective or dual PI3K p110 inhibitors and this might be due to the presence of gain-of-function PI3K mutations in this cell line. In particular, REH cells carry mutations in *PI3KR1*, *PIK3CG* and *PIK3CD* genes (encoding the regulatory p85α, p110γ and p110δ catalytic subunits, respectively) according to the COSMIC database (http://cancer.sanger.ac.uk/cell_lines/sample/overview?id=909696).

We have also shown that ZSTK-474 and IPI-145 could inhibit the *in vitro* motility of B-ALL cells. It has been demonstrated that migration mediated by CXCL12/CXCR4 axis is associated with relapses and a bad patient outcome in B-ALL patients (Bruggemann et al., 2012). Moreover, chemokines, such as CXCL12, secreted by stromal cells in the bone marrow microenvironment, increase leukemic survival and GC resistance (Randhawa et al., 2016) and our results, obtained by co-culturing NALM6 and REH cells with hBMSCs, are consistent with these recent observations.

As GCs are used for the treatment of B-ALL, we wanted to analyze the effects of PI3K p110 inhibitors on DEX response. In particular, both ZSTK-474 and IPI-145 strongly synergized with

DEX in all tested cell lines and in samples treated with PI3K p110 inhibitors + DEX combination an increased GC-induced apoptosis was observed in both GC-sensitive and -resistant cell lines.

GC-induced cell death depends on the interactions between the hormone and the cytosolic GR that mediates apoptosis induction. Multiple mechanisms are responsible for GC resistance, including decreased expression of GR, altered affinity of GR for its ligand and dysregulation of GR nuclear translocation (Azher et al., 2016; Bhadri et al., 2012). In particular, it seems that this latter process is controlled by PI3K/Akt/mTOR signaling. Indeed, phosphorylation of GR at Ser134 by Akt causes an impairment of GR translocation in T-ALL cells (Piovan et al., 2013) and this phenomenon could be particularly relevant in cells which display a hyper-activated PI3K/Akt/mTOR cascade, such as B-ALL cells.

We demonstrated that single treatment with either PI3K p110 inhibitors (ZSTK-474 and IPI-145) or DEX, did not lead to GR nuclear translocation in KOPN8 and NALM6 cells, however translocation could be induced by treating cells with drug combinations. Moreover, we demonstrated that both ZSTK-474 and IPI-145 caused a de-phosphorylation of Ser134 p-GR and a rescue of GCs response, in agreement with what was documented by Piovan et al. in T-ALL cells (Piovan et al., 2013).

An association between the modulation of specific anti-apoptotic and pro-apoptotic proteins, such as Mcl-1 and Bim, and GCs resistance has been proposed in pediatric B-ALL (Holleman et al., 2006; Jiang et al., 2011). In addition, it has been demonstrated that rapamycin, an mTOR inhibitor, induced GC sensitivity in primary ALL samples via Mcl-1 modulation (Wei et al., 2006). Interestingly, Wei et al. demonstrated that even a weak decrease in Mcl-1 expression could have a significant effect on regulation of apoptotic intrinsic pathway (Wei et al., 2006). We demonstrated that DEX + IPI-145 and DEX + ZSTK-474 combinations modulated Mcl-1 and Bim expression levels, suggesting that this could be another mechanism through which PI3K p110 inhibitors may restore GC sensitivity.

The synergism between ZSTK-474 and DEX was examined in more depth by means of gene expression analysis in NALM6 cells.

Remarkably, ZSTK-474 potentiated the DEX-induced up- and down-regulation of genes that are involved in the complex process of GC-dependent apoptosis. In agreement with the literature data, DEX induced a rapid and marked increase in *TSC22D3* expression, a master regulator of GC anti-proliferative, pro-apoptotic and anti-inflammatory effects (Bruscoli et al., 2015), and this increase was strengthened by the addition of ZSTK-474 (a further 2.5 fold increase in *TSC22D3* mRNA compared to samples treated with DEX alone).

Interestingly, on one hand ZSTK-474 seemed to reinforce the ability of DEX to down-regulate genes which are involved in proliferation, survival and anti-apoptotic mechanisms such as *BCL6, CEBPB, COL4A2, CREB3, PIK3R1, POU2F2, SPHK1, STAT5B, USP2,* on the other, ZSTK-474 rescued the effects of some genes involved in tumor progression and most likely also in GC-resistance such as *AQP1, CTGF, DDIT4, FKBP5* and *IL10*.

Indeed, the immunomodulatory cytokine interleukin-10 (IL10) is frequently found up-regulated in various types of cancer and can be produced by tumor cells, thus contributing to tolerance and tumor-escape processes (Mannino et al., 2015). *AQP1* and *CTGF*, a water channel protein and a growth factor respectively, participate in cell growth and migration processes (Chu et al., 2008; Papadopoulos et al., 2008). Finally, ZSTK-474 caused an increase in *RGS2* and *SESN1* expression, which are negative regulators of MAP kinase and mTOR signaling, respectively (Chantranupong et al., 2014; Nguyen et al., 2009).

However, it is essential to consider that the combined treatment also up-regulated some anti-apoptotic and/or pro-inflammatory genes, such as *IL6, RASA3* and *SGK1*. Although these findings have been obtained using only a single cell line and need to be validated in primary samples, we think that they are important as they highlighted some genes that could blunt the efficacy of a targeted therapy based on PI3K inhibitors in B-ALL cells.

As to the toxicity of PI3K p110 inhibitors on $CD19^+$ peripheral blood B-lymphocytes from healthy donors, our unpublished data documented that ZTSK-474, even when employed at the maximal concentration of 10 μM, was less cytotoxic to normal than to neoplastic B-cells, as about 70% of B-

lymphocytes were still viable. Regarding IPI-145, several lines of evidence indicate that this drug does not affect the viability of normal B-cells (Balakrishnan et al., 2015; Dong et al., 2014; Gockeritz et al., 2015).

Others inhibitors of the PI3K/Akt/mTOR pathway have been tested in combination with GCs in preclinical models of ALL, including rapamycin, an allosteric mTORC1 inhibitor, (Zhang et al., 2012), and MK2206, an allosteric Akt inhibitor, (Piovan et al., 2013). However, clinical trials, performed with these inhibitors in acute leukemia patients, have provided quite disappointing results (Konopleva et al., 2014; Perl et al., 2009). Therefore, new drugs targeting this pathway, including PI3K p110 inhibitors, should be tested.

In conclusion, our findings strongly advocate the use of PI3K p110 inhibitors for improving the clinical outcome of pediatric B-ALL patients. A pan PI3K p110 inhibitor displayed the most powerful cytotoxic effects and synergized with DEX. However, also a dual γ/δ PI3K p110 inhibitor was effective in combination with DEX, even when used on DEX-resistant cells. Therefore, IPI-145 could have a clinical relevance not only for B-ALL patients that respond to GCs by decreasing the drug dosage needed and adverse effects, but also for patients who do not respond to GCs. Moreover, the use of a dual inhibitor could spare the patients the side effects elicited by the inhibition of all the four PI3K p110 catalytic subunits (Greenwell et al., 2017).

Literature Cited

Aries IM, Jerchel IS, van den Dungen RE, van den Berk LC, Boer JM, Horstmann MA, Escherich G, Pieters R, den Boer ML. 2014. EMP1, a novel poor prognostic factor in pediatric leukemia regulates prednisolone resistance, cell proliferation, migration and adhesion. Leukemia 28:1828-1837.

Azher S, Azami O, Amato C, McCullough M, Celentano A, Cirillo N. 2016. The non-conventional effects of glucocorticoids in cancer. J Cell Physiol 231:2368-2373.

Bachmann PS, Gorman R, Mackenzie KL, Lutze-Mann L, Lock RB. 2005. Dexamethasone resistance in B-cell precursor childhood acute lymphoblastic leukemia occurs downstream of ligand-induced nuclear translocation of the glucocorticoid receptor. Blood 105:2519-2526.

Balakrishnan K, Peluso M, Fu M, Rosin NY, Burger JA, Wierda WG, Keating MJ, Faia K, O'Brien S, Kutok JL, Gandhi V. 2015. The phosphoinositide-3-kinase (PI3K)-δ and γ inhibitor, IPI-145 (Duvelisib), overcomes signals from the PI3K/AKT/S6 pathway and promotes apoptosis in CLL. Leukemia 29:1811-1822.

Bhadri VA, Trahair TN, Lock RB. 2012. Glucocorticoid resistance in paediatric acute lymphoblastic leukaemia. J Paediatr Child Health 48:634-640.

Bradstock KF, Makrynikola V, Bianchi A, Shen W, Hewson J, Gottlieb DJ. 2000. Effects of the chemokine stromal cell-derived factor-1 on the migration and localization of precursor-B acute lymphoblastic leukemia cells within bone marrow stromal layers. Leukemia 14:882-888.

Bruggemann M, Raff T, Kneba M. 2012. Has MRD monitoring superseded other prognostic factors in adult ALL? Blood 120:4470-4481.

Bruscoli S, Biagioli M, Sorcini D, Frammartino T, Cimino M, Sportoletti P, Mazzon E, Bereshchenko O, Riccardi C. 2015. Lack of glucocorticoid-induced leucine zipper (GILZ) deregulates B-cell survival and results in B-cell lymphocytosis in mice. Blood 126:1790-1801.

Burger JA, Peled A. 2009. CXCR4 antagonists: targeting the microenvironment in leukemia and other cancers. Leukemia 23:43-52.

Camps M, Ruckle T, Ji H, Ardissone V, Rintelen F, Shaw J, Ferrandi C, Chabert C, Gillieron C, Francon B, Martin T, Gretener D, Perrin D, Leroy D, Vitte PA, Hirsch E, Wymann MP, Cirillo R, Schwarz MK, Rommel C. 2005. Blockade of PI3Kγ suppresses joint inflammation and damage in mouse models of rheumatoid arthritis. Nat Med 11:936-943.

Chantranupong L, Wolfson RL, Orozco JM, Saxton RA, Scaria SM, Bar-Peled L, Spooner E, Isasa M, Gygi SP, Sabatini DM. 2014. The Sestrins interact with GATOR2 to negatively regulate the amino-acid-sensing pathway upstream of mTORC1. Cell Rep 9:1-8.

Chantry D, Vojtek A, Kashishian A, Holtzman DA, Wood C, Gray PW, Cooper JA, Hoekstra MF. 1997. p110δ, a novel phosphatidylinositol 3-kinase catalytic subunit that associates with p85 and is expressed predominantly in leukocytes. J Biol Chem 272:19236-19241.

Chou TC, Talalay P. 1984. Quantitative analysis of dose-effect relationships: the combined effects of multiple drugs or enzyme inhibitors. Adv Enzyme Regul 22:27-55.

Chu CY, Chang CC, Prakash E, Kuo ML. 2008. Connective tissue growth factor (CTGF) and cancer progression. J Biomed Sci 15:675-685.

Curran E, Smith SM. 2014. Phosphoinositide 3-kinase inhibitors in lymphoma. Curr Opin Oncol 26:469-475.

Den Boer ML, Harms DO, Pieters R, Kazemier KM, Gobel U, Korholz D, Graubner U, Haas RJ, Jorch N, Spaar HJ, Kaspers GJ, Kamps WA, Van der Does-Van den Berg A, Van Wering ER, Veerman AJ, Janka-Schaub GE. 2003. Patient stratification based on prednisolone-vincristine-asparaginase resistance profiles in children with acute lymphoblastic leukemia. J Clin Oncol 21:3262-3268.

Dong S, Guinn D, Dubovsky JA, Zhong Y, Lehman A, Kutok J, Woyach JA, Byrd JC, Johnson AJ. 2014. IPI-145 antagonizes intrinsic and extrinsic survival signals in chronic lymphocytic leukemia cells. Blood 124:3583-3586.

Engelman JA, Luo J, Cantley LC. 2006. The evolution of phosphatidylinositol 3-kinases as regulators of growth and metabolism. Nat Rev Genet 7:606-619.

Frolova O, Samudio I, Benito JM, Jacamo R, Kornblau SM, Markovic A, Schober W, Lu H, Qiu YH, Buglio D, McQueen T, Pierce S, Shpall E, Konoplev S, Thomas D, Kantarjian H, Lock R, Andreeff M, Konopleva M. 2012. Regulation of HIF-1α signaling and chemoresistance in acute lymphocytic leukemia under hypoxic conditions of the bone marrow microenvironment. Cancer Biol Ther 13:858-870.

Fruman DA, Rommel C. 2014. PI3K and cancer: lessons, challenges and opportunities. Nat Rev Drug Discov 13:140-156.

Fuka G, Kantner HP, Grausenburger R, Inthal A, Bauer E, Krapf G, Kaindl U, Kauer M, Dworzak MN, Stoiber D, Haas OA, Panzer-Grumayer R. 2012. Silencing of ETV6/RUNX1 abrogates PI3K/AKT/mTOR signaling and impairs reconstitution of leukemia in xenografts. Leukemia 26:927-933.

Galliher-Beckley AJ, Williams JG, Cidlowski JA. 2011. Ligand-independent phosphorylation of the glucocorticoid receptor integrates cellular stress pathways with nuclear receptor signaling. Mol Cell Biol 31:4663-4675.

Gockeritz E, Kerwien S, Baumann M, Wigger M, Vondey V, Neumann L, Landwehr T, Wendtner CM, Klein C, Liu N, Hallek M, Frenzel LP, Krause G. 2015. Efficacy of phosphatidylinositol-3 kinase inhibitors with diverse isoform selectivity profiles for inhibiting the survival of chronic lymphocytic leukemia cells. Int J Cancer 137:2234-2242.

Gomes AM, Soares MV, Ribeiro P, Caldas J, Povoa V, Martins LR, Melao A, Serra-Caetano A, de Sousa AB, Lacerda JF, Barata JT. 2014. Adult B-cell acute lymphoblastic leukemia cells

display decreased PTEN activity and constitutive hyperactivation of PI3K/Akt pathway despite high PTEN protein levels. Haematologica 99:1062-1068.

Graux C. 2011. Biology of acute lymphoblastic leukemia (ALL): clinical and therapeutic relevance. Transfus Apher Sci 44:183-189.

Greenwell IB, Flowers CR, Blum KA, Cohen JB. 2017. Clinical use of PI3K inhibitors in B-cell lymphoid malignancies: today and tomorrow. Expert Rev Anticancer Ther 17:271-279.

Guest EM, Stam RW. 2017. Updates in the biology and therapy for infant acute lymphoblastic leukemia. Curr Opin Pediatr 29:20-26.

Hanahan D, Weinberg RA. 2011. Hallmarks of cancer: the next generation. Cell 144(5):646-674.

Harned TM, Gaynon P. 2008. Relapsed acute lymphoblastic leukemia: current status and future opportunities. Curr Oncol Rep 10:453-458.

He B, Zhang N, Zhao R. 2016. Dexamethasone downregulates SLC7A5 expression and promotes cell cycle arrest, autophagy and apoptosis in BeWo cells. J Cell Physiol 231:233-242.

Herman SE, Gordon AL, Wagner AJ, Heerema NA, Zhao W, Flynn JM, Jones J, Andritsos L, Puri KD, Lannutti BJ, Giese NA, Zhang X, Wei L, Byrd JC, Johnson AJ. 2010. Phosphatidylinositol 3-kinase-δ inhibitor CAL-101 shows promising preclinical activity in chronic lymphocytic leukemia by antagonizing intrinsic and extrinsic cellular survival signals. Blood 116:2078-2088.

Hirai H, Sootome H, Nakatsuru Y, Miyama K, Taguchi S, Tsujioka K, Ueno Y, Hatch H, Majumder PK, Pan BS, Kotani H. 2010. MK-2206, an allosteric Akt inhibitor, enhances antitumor efficacy by standard chemotherapeutic agents or molecular targeted drugs in vitro and in vivo. Mol Cancer Ther 9:1956-1967.

Holleman A, Cheok MH, den Boer ML, Yang W, Veerman AJ, Kazemier KM, Pei D, Cheng C, Pui CH, Relling MV, Janka-Schaub GE, Pieters R, Evans WE. 2004. Gene-expression patterns in drug-resistant acute lymphoblastic leukemia cells and response to treatment. N Engl J Med 351:533-542.

Holleman A, den Boer ML, de Menezes RX, Cheok MH, Cheng C, Kazemier KM, Janka-Schaub GE, Gobel U, Graubner UB, Evans WE, Pieters R. 2006. The expression of 70 apoptosis genes in relation to lineage, genetic subtype, cellular drug resistance, and outcome in childhood acute lymphoblastic leukemia. Blood 107:769-776.

Huang CY, Hsieh NT, Li CI, Weng YT, Liu HS, Lee MF. 2017. MED28 regulates epithelial-mesenchymal transition through NFκB in Human Breast Cancer Cells. J Cell Physiol 232:1337-1345.

Inaba H, Pui CH. 2010. Glucocorticoid use in acute lymphoblastic leukaemia. Lancet Oncol 11:1096-1106.

Jiang N, Koh GS, Lim JY, Kham SK, Ariffin H, Chew FT, Yeoh AE. 2011. BIM is a prognostic biomarker for early prednisolone response in pediatric acute lymphoblastic leukemia. Exp Hematol 39:321-329, 329 e321-323.

Jing D, Bhadri VA, Beck D, Thoms JA, Yakob NA, Wong JW, Knezevic K, Pimanda JE, Lock RB. 2015. Opposing regulation of BIM and BCL2 controls glucocorticoid-induced apoptosis of pediatric acute lymphoblastic leukemia cells. Blood 125:273-283.

Kaspers GJ, Pieters R, Van Zantwijk CH, Van Wering ER, Van Der Does-Van Den Berg A, Veerman AJ. 1998. Prednisolone resistance in childhood acute lymphoblastic leukemia: vitro-vivo correlations and cross-resistance to other drugs. Blood 92:259-266.

Khwaja A. 2010. PI3K as a target for therapy in haematological malignancies. Curr Top Microbiol Immunol 347:169-188.

Konoplev S, Jorgensen JL, Thomas DA, Lin E, Burger J, Kantarjian HM, Andreeff M, Medeiros LJ, Konopleva M. 2011. Phosphorylated CXCR4 is associated with poor survival in adults with B-acute lymphoblastic leukemia. Cancer 117:4689-4695.

Konopleva MY, Walter RB, Faderl SH, Jabbour EJ, Zeng Z, Borthakur G, Huang X, Kadia TM, Ruvolo PP, Feliu JB, Lu H, Debose L, Burger JA, Andreeff M, Liu W, Baggerly KA, Kornblau SM, Doyle LA, Estey EH, Kantarjian HM. 2014. Preclinical and early clinical evaluation of the oral AKT inhibitor, MK-2206, for the treatment of acute myelogenous leukemia. Clin Cancer Res 20:2226-2235.

Laplante M, Sabatini DM. 2012. mTOR signaling in growth control and disease. Cell 149:274-293.

Li L, Lou Z, Wang L. 2011. The role of FKBP5 in cancer aetiology and chemoresistance. Br J Cancer 104:19-23.

Lonetti A, Cappellini A, Sparta AM, Chiarini F, Buontempo F, Evangelisti C, Orsini E, McCubrey JA, Martelli AM. 2015. PI3K pan-inhibition impairs more efficiently proliferation and survival of T-cell acute lymphoblastic leukemia cell lines when compared to isoform-selective PI3K inhibitors. Oncotarget 6:10399-10414.

Mannino MH, Zhu Z, Xiao H, Bai Q, Wakefield MR, Fang Y. 2015. The paradoxical role of IL-10 in immunity and cancer. Cancer Lett 367:103-107.

Miller SM, Goulet DR, Johnson GL. 2017. Targeting the breast cancer kinome. J Cell Physiol 232:53-60.

Morishita N, Tsukahara H, Chayama K, Ishida T, Washio K, Miyamura T, Yamashita N, Oda M, Morishima T. 2012. Activation of Akt is associated with poor prognosis and chemotherapeutic resistance in pediatric B-precursor acute lymphoblastic leukemia. Pediatr Blood Cancer 59:83-89.

Nguyen CH, Ming H, Zhao P, Hugendubler L, Gros R, Kimball SR, Chidiac P. 2009. Translational control by RGS2. J Cell Biol 186:755-765.

Norman M, Hearing SD. 2002. Glucocorticoid resistance - what is known? Curr Opin Pharmacol 2:723-729.

Papadopoulos MC, Saadoun S, Verkman AS. 2008. Aquaporins and cell migration. Pflugers Arch 456:693-700.

Perl AE, Kasner MT, Tsai DE, Vogl DT, Loren AW, Schuster SJ, Porter DL, Stadtmauer EA, Goldstein SC, Frey NV, Nasta SD, Hexner EO, Dierov JK, Swider CR, Bagg A, Gewirtz AM, Carroll M, Luger SM. 2009. A phase I study of the mammalian target of rapamycin inhibitor sirolimus and MEC chemotherapy in relapsed and refractory acute myelogenous leukemia. Clin Cancer Res 15:6732-6739.

Piovan E, Yu J, Tosello V, Herranz D, Ambesi-Impiombato A, Da Silva AC, Sanchez-Martin M, Perez-Garcia A, Rigo I, Castillo M, Indraccolo S, Cross JR, de Stanchina E, Paietta E, Racevskis J, Rowe JM, Tallman MS, Basso G, Meijerink JP, Cordon-Cardo C, Califano A, Ferrando AA. 2013. Direct reversal of glucocorticoid resistance by AKT inhibition in acute lymphoblastic leukemia. Cancer Cell 24:766-776.

Polak R, Buitenhuis M. 2012. The PI3K/PKB signaling module as key regulator of hematopoiesis: implications for therapeutic strategies in leukemia. Blood 119:911-923.

Poli A, Fiume R, Baldanzi G, Capello D, Ratti S, Gesi M, Manzoli L, Graziani A, Suh PG, Cocco L, Follo MY. 2017. Nuclear localization of diacylglycerol kinase α in K562 cells is involved in cell cycle progression. J Cell Physiol 232:2550-2557.

Pui CH, Evans WE. 2006. Treatment of acute lymphoblastic leukemia. N Engl J Med 354:166-178.

Ramazzotti G, Bavelloni A, Blalock W, Piazzi M, Cocco L, Faenza I. 2016. BMP-2 induced expression of PLCβ1 that is a positive regulator of osteoblast differentiation. J Cell Physiol 231:623-629.

Randhawa S, Cho BS, Ghosh D, Sivina M, Koehrer S, Muschen M, Peled A, Davis RE, Konopleva M, Burger JA. 2016. Effects of pharmacological and genetic disruption of CXCR4 chemokine receptor function in B-cell acute lymphoblastic leukaemia. Br J Haematol 174:425-436.

Shrestha A, Nepal S, Kim MJ, Chang JH, Kim SH, Jeong GS, Jeong CH, Park GH, Jung S, Lim J, Cho E, Lee S, Park PH. 2016. Critical role of AMPK/FoxO3A axis in globular adiponectin-induced cell cycle arrest and apoptosis in cancer cells. J Cell Physiol 231:357-369.

Siegel R, Naishadham D, Jemal A. 2012. Cancer statistics, 2012. CA Cancer J Clin 62:10-29.

Silva A, Yunes JA, Cardoso BA, Martins LR, Jotta PY, Abecasis M, Nowill AE, Leslie NR, Cardoso AA, Barata JT. 2008. PTEN posttranslational inactivation and hyperactivation of the PI3K/Akt pathway sustain primary T cell leukemia viability. J Clin Invest 118:3762-3774.

Sofer A, Lei K, Johannessen CM, Ellisen LW. 2005. Regulation of mTOR and cell growth in response to energy stress by REDD1. Mol Cell Biol 25:5834-5845.

Spijkers-Hagelstein JA, Pinhancos SS, Schneider P, Pieters R, Stam RW. 2014. Chemical genomic screening identifies LY294002 as a modulator of glucocorticoid resistance in MLL-rearranged infant ALL. Leukemia 28:761-769.

Stengel C, Jenner E, Meja K, Mayekar S, Khwaja A. 2013. Proliferation of PTEN-deficient haematopoietic tumour cells is not affected by isoform-selective inhibition of p110 PI3-kinase and requires blockade of all class 1 PI3K activity. Br J Haematol 162:285-289.

Subramaniam PS, Whye DW, Efimenko E, Chen J, Tosello V, De Keersmaecker K, Kashishian A, Thompson MA, Castillo M, Cordon-Cardo C, Dave UP, Ferrando A, Lannutti BJ, Diacovo TG. 2012. Targeting nonclassical oncogenes for therapy in T-ALL. Cancer Cell 21:459-472.

Tang N, Lyu D, Liu T, Chen F, Jing S, Hao T, Liu S. 2016. Different Effects of p52SHC1 and p52SHC3 on the Cell Cycle of Neurons and Neural Stem Cells. J Cel Physiol 231:172-180.

Tasian SK, Teachey DT, Rheingold SR. 2014. Targeting the PI3K/mTOR pathway in pediatric hematologic malignancies. Front Oncol 4:108.

Teicher BA, Fricker SP. 2010. CXCL12 (SDF-1)/CXCR4 pathway in cancer. Clin Cancer Res 16:2927-2931.

van den Berk LC, van der Veer A, Willemse ME, Theeuwes MJ, Luijendijk MW, Tong WH, van der Sluis IM, Pieters R, den Boer ML. 2014. Disturbed CXCR4/CXCL12 axis in paediatric precursor B-cell acute lymphoblastic leukaemia. Br J Haematol 166:240-249.

Wei G, Twomey D, Lamb J, Schlis K, Agarwal J, Stam RW, Opferman JT, Sallan SE, den Boer ML, Pieters R, Golub TR, Armstrong SA. 2006. Gene expression-based chemical genomics identifies rapamycin as a modulator of MCL1 and glucocorticoid resistance. Cancer Cell 10:331-342.

Whitfield GK, Jurutka PW, Haussler CA, Haussler MR. 1999. Steroid hormone receptors: evolution, ligands, and molecular basis of biologic function. J Cell Biochem Suppl 32-33:110-122.

Zhang C, Ryu YK, Chen TZ, Hall CP, Webster DR, Kang MH. 2012. Synergistic activity of rapamycin and dexamethasone in vitro and in vivo in acute lymphoblastic leukemia via cell-cycle arrest and apoptosis. Leuk Res 36:342-349.

Figure legends

Fig. 1. PI3K p110 inhibitors affect viability of B-ALL cell lines. A) Western blotting analysis. Cells were collected, lysed, and analyzed by western blotting. **B)** MTT assays were performed on B-ALL cell lines after 24 hours of treatment with ZSTK-474, AS-605240 (AS), CAL-101 (CAL), AS-605240+CAL-101 (CAL-101) and IPI-145. The results are the mean of at least three different experiments ± s.d.

Fig. 2. PI3K p110 inhibitors affect cycle progression, induce apoptosis and down-regulate migration of B-ALL cell lines. A) B-ALL cell lines were treated for 24 hours with 5 μM of the following drugs: ZSTK-474 (ZSTK), AS-605240 (AS), CAL-101 (CAL), AS-605240+CAL-101 (AS+CAL), IPI-145 (IPI). Cell cycle analysis was then performed by flow cytometry. CTR: untreated cells. ∗ $p<0.05$ relative to CTR. **B)** B-ALL cell lines were treated for 24 hours with 5 μM of the following drugs: ZSTK-474 (ZSTK), AS-605240 (AS), CAL-101 (CAL), AS-605240+CAL-101 (AS+CAL), IPI-145 (IPI). Then, cells were stained with Annexin V-FITC/PI and analyzed by flow cytometry. CTR: untreated cells. ∗ $p<0.05$ relative to CTR. **C)** REH cells were assayed for apoptosis by Annexin V-FITC/PI staining upon treatment for 24 hours with 5 μM of the following drugs ZSTK-474 (ZSTK), AS-605240 (AS), CAL-101 (CAL), AS-605240+CAL-101 (AS+CAL), IPI-145 (IPI). Results from a representative experiment are shown. CTR: untreated cells. **D)** Western blotting analysis documenting caspase 3 and PARP cleavage in response to PI3K inhibitor treatment (5 μM for 24 hours). CTR: untreated cells. **E)** B-ALL cell lines were treated with 5 μM of either ZSTK-474 (ZSTK) or IPI-145. Migration towards the chemoattractant agent CXCL12 (200 ng/ml) was tested using a Transwell$^{@}$ system as described in "Materials and Methods". After 4 hours of drug treatment, transmigrated cells were recovered and counted under the microscope. CTR: untreated cells. ∗ $p<0.05$ relative to CTR.

Fig. 3. ZSTK-474 is the most effective drug in down-regulating the PI3K/Akt/mTOR signaling pathway. A) Flow cytometric analysis of PtdIns 3,4,5P_3 levels in B-ALL cells treated with 5 μM of either ZSTK-474 (ZSTK) or IPI-145 (IPI). CTR: untreated cells. ∗ $p<0.05$ relative to CTR. **B)** B-ALL cell lines were treated for 4 hours with 5 μM of the following drugs: ZSTK-474 (ZSTK), AS-605240 (AS), CAL-101 (CAL), AS-605240+CAL-101 (AS+CAL), IPI-145 (IPI). Then, cells were collected, lysed and analyzed by western blotting. Dephosphorylation of Akt and S6RP was induced by PI3K inhibitors, especially by ZSTK-474. CTR: untreated cells.

Fig. 4. **PI3K p110 inhibitors and DEX display synergistic effects in B-ALL cells. A)** Cells were incubated for 24 hours with increasing concentrations of DEX, then MTT assays were performed. **B)** MTT assays of B-ALL cells treated for 24 hours with PI3K inhibitors alone or in combination with DEX at a fixed ratio (DEX : PI3K p110 inhibitor, 1:50). ZSTK-474 (ZSTK), AS-605240 (AS), CAL-101 (CAL), AS-605240+CAL-101 (AS+CAL), IPI-145 (IPI). In A and B results are the mean of at least three different experiments ± s.d.

Fig. 5. DEX enhances apoptosis induced by PI3K p110 inhibitors in B-ALL cells. A) B-ALL cell lines were treated for 24 hours with DEX (0.1 μM), ZSTK-474 (ZSTK, 5 μM), AS-605240 (AS, 5 μM), CAL-101 (CAL, 5 μM), AS-605240 + CAL-101 (AS + CAL, both at 5 μM), IPI-145 (IPI, 5 μM), alone, or with a combination of the PI3K p110 inhibitors with DEX at the same concentrations as above. Then, Annexin V-FITC/PI staining analysis was performed by flow cytometry. CTR: untreated cells. ∗ $p<0.05$ relative to CTR. **B)** B-ALL cell lines were treated for 24 hours with DEX (0.1 μM), IPI-145 (IPI, 5 μM), ZSTK-474 (ZSTK, 5 μM) alone, with a combination of the PI3K p110 inhibitors with DEX at the same concentrations as above. Then, western blot analysis for caspase 3 and PARP cleavage was performed. CTR: untreated cells. **C)** Western blotting analysis documenting Mcl-1 and Bim expression after treatment for 24 hours with

DEX (0.1 μM), IPI-145 (IPI, 5 μM) or ZSTK-145 (ZSTK, 5 μM) or their combinations at the same concentrations. CTR: untreated cells. Band intensities were quantified by NIH Image J densitometry analysis. The values represent the amount of protein present in treated samples relative to untreated cells after normalizing to β-actin density. CTR: untreated cells.

Fig. 6. PI3K p110 inhibitors lower hBMSC-induced DEX-resistance in B-ALL cell lines. A) hBMSC were treated for 48 hours with DEX (0.1 μM), IPI-145 (IPI, 5 μM) or ZSTK-474 (ZSTK, 5 μM). CTR: untreated cells. Cell viability was then measured by MTT assays. The results are the mean of three different experiments ± s.d. **B)** PI3K p110 inhibitors sensitize B-ALL cell lines to DEX. Cell viability was analyzed by MTT assays, 48 hours after treatment with DEX (0.1 μM) in either the absence or the presence of hBMSCs, using a Transwell$^{@}$ system. IPI-145 (IPI) and ZSTK-474 (ZSTK) were used at 5 μM. CTR: untreated cells. The results are the mean of three different experiments ± s.d. Asterisks indicate statistically significant differences with respect to samples cultured without hBMSC ($p < 0.05$).

Fig. 7. **PI3K p110 inhibitors induce GR nuclear translocation in B-ALL cells. A)** GR protein expression in B-ALL cell lines as assessed by western blot analysis. **B)** Western blotting analysis showing Ser134 p-GR levels in B-ALL cell lines treated for 4 hours with 0.1 μM DEX, 5 μM IPI-145 (IPI), 5 μM ZSTK-454 (ZSTK), or 2 μM MK2206. **C)** Immunofluorescence detection of GR nuclear translocation in NALM6 and KOPN8 cells. Cells were treated for 4 hours with DEX (0.1 μM), IPI-145 (IPI, 5 μM), ZSTK-474 (ZSTK, 5 μM) or their combinations at the same concentrations. Cells were labeled using an antibody to GR which was revealed by a FITC-conjugated secondary antibody (green). Slides were counterstained with DAPI to visualize nuclei (blue). A translocation of GR from cytoplasm to the nucleus was observed in response to combined treatments (DEX + IPI-145, or DEX + ZSTK-474). Fields shown are representative of at least 5

imaged fields. Scale bar: 10 μm. **D)** Subcellular fractionation to detect nuclear translocation of GR protein in NALM6 cells. Cells were treated for 4 hours with DEX (0.1 μM), IPI-145 (IPI, 5 μM), ZSTK-474 (ZSTK, 5 μM) or their combinations at the same concentrations. Equal amounts of protein (30 μg) from cytoplasmic (Cyt) and nuclear (N) fractions were separated by SDS-PAGE. Membranes were probed with antibodies to GR, β-actin (cytoplasmic marker), and histone H3 (nuclear marker). Western blot analysis confirmed the nuclear translocation of GR in response to the combined treatments. CTR: untreated cells.

Fig. 8. ZSTK-474 affects the expression of several GC-related genes in NALM6 cells.

A real-time PCR expression profiling of 82 GC-related genes was performed in NALM6 cells after 8 hours of treatment with DEX (0.1 μM), ZSTK-474 (ZSTK, 5 μM) alone or in combination at the same concentrations. **A)** Histogram shows differently expressed genes (fold-change ≥ 2) versus untreated (CTR) samples. Results are the mean of three separate experiments ± s.d. **B)** Histograms show differentially expressed genes in DEX + ZSTK-474 versus DEX only samples. Results are the mean of three separate experiments ± s.d. CTR: untreated samples.

Figure 9. Combination of PI3K p110 inhibitors with DEX is cytotoxic to B-ALL primary cells.

A) MTT assays performed on B-ALL patient samples treated for 24 hours with increasing concentrations of DEX, IPI-145 (IPI), ZSTK-474 (ZSTK) or their combinations at a fixed ratio PI3K inhibitor : DEX, 50:1. The results are the mean of four different B-ALL patients ± s.d. Each patients was analyzed twice. **B)** Flow cytometric analysis of two representative patient samples treated for 24 hours with DEX (0.1 μM), IPI-145 (IPI, 5 μM), ZSTK-474 (ZSTK, 5 μM) or their combinations at the same concentrations. Cells were stained with Annexin V-FITC/PI. CTR: untreated cells. **C)** Western blot analysis of a representative patient sample treated for 24 hours with DEX (0.1 μM), IPI-145 (IPI, 5 μM), ZSTK-474 (ZSTK, 5 μM) or their combinations at the same

concentrations. Twenty µg of protein was electrophoresed on SDS-PAGE, transferred to a nitrocellulose membrane and probed with the appropriate antibodies. CTR: untreated cells.

Table 1. IC_{50} values obtained by MTT assays after a 24 hour treatment with increasing concentrations of drugs (μM). N.D.: not determined. AS-605240 + CAL-101: AS+CAL.

	KOPN8	**NALM6**	**REH**
ZSTK-474	4.9	0.1	0.1
AS-605240	N.D.	N.D.	7.9
CAL-101	>10	N.D.	7.5
AS+CAL	>10	N.D.	3.1
IPI-145	N.D.	>10	2.6

Table 2. Analysis of the effects of DEX treatment combined with PI3K p110 inhibitors in B-ALL cell lines. PI3K inhibitor : DEX ratio was 50 :1. Combination index (CI) values, calculated with the CalcuSyn software, are presented. ZSTK-474: ZSTK; AS-605240: AS; CAL-101: CAL; AS-605240+CAL-101: AS+CAL; IPI-145: IPI.

KOPN8

	CI				
[μM]	**ZSTK+DEX**	**AS+DEX**	**CAL+DEX**	**AS+CAL+DEX**	**IPI+DEX**
0.0065/0.3125	0.28	0.68	0.69	0.15	0.05
0.025/1.25	0.26	0.79	0.77	0.20	0.01
0.1/5	0.39	1.77	0.82	0.47	0.02
0.2/10	0.44	1.16	0.71	0.58	0.04

NALM6

	CI				
[μM]	**ZSTK+DEX**	**AS+DEX**	**CAL+DEX**	**AS+CAL+DEX**	**IPI+DEX**
0.0065/0.3125	0.43	1.33	0.35	0.88	0.41
0.025/1.25	0.39	0.76	0.33	0.27	0.19
0.1/5	0.55	0.48	0.39	0.26	0.22
0.2/10	0.43	0.71	0.49	0.33	0.24

REH

	CI				
[μM]	**ZSTK+DEX**	**AS+DEX**	**CAL+DEX**	**AS+CAL+DEX**	**IPI+DEX**
0.0065/0.3125	0.43	0.93	0.52	1.01	0.57
0.025/1.25	0.16	1.24	0.70	0.70	0.25
0.1/5	0.17	0.82	0.65	0.87	0.21
0.2/10	0.19	1.10	0.93	0.85	0.22

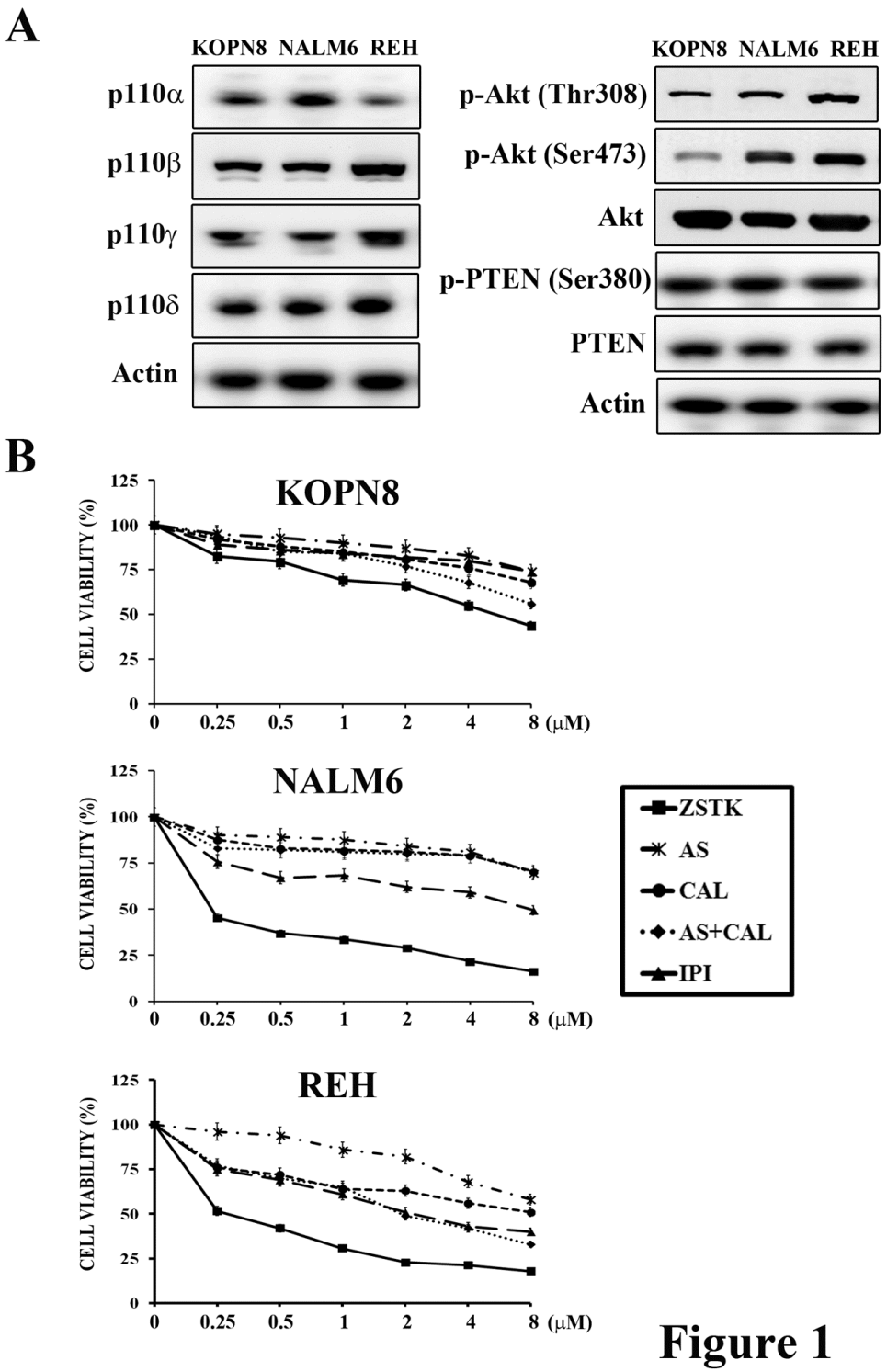
A
KOPN8 NALM6 REH
p110α
p110β
p110γ
p110δ
Actin
KOPN8 NALM6 REH
p-Akt (Thr308)
p-Akt (Ser473)
Akt
p-PTEN (Ser380)
PTEN
Actin
B
KOPN8
NALM6
REH
CELL VIABILITY (%)
125
100
75
50
25
0
0 0.25 0.5 1 2 4 8 (μM)
ZSTK
AS
CAL
AS+CAL
IPI

Figure 1

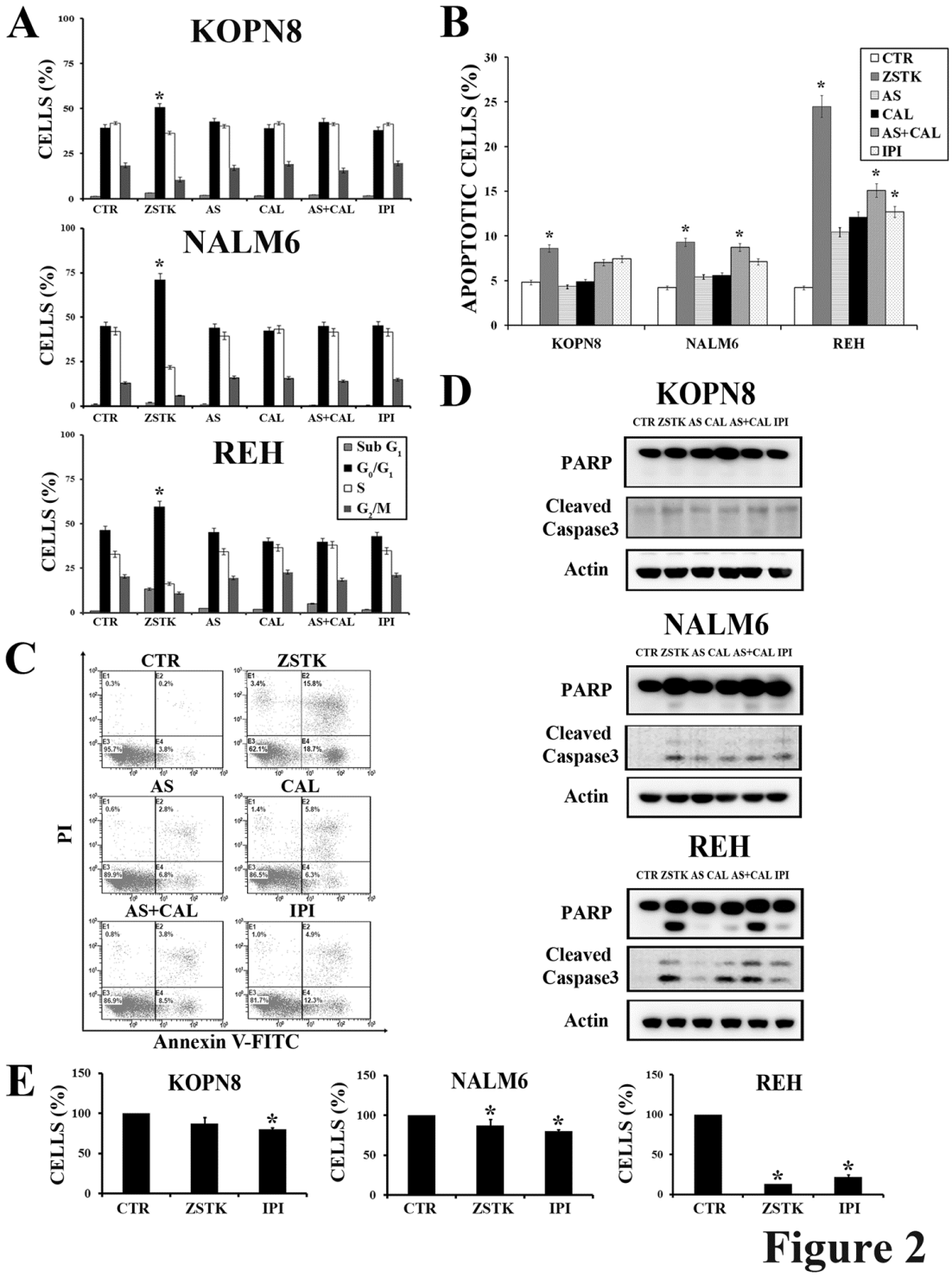
A
KOPN8
NALM6
REH
CELLS (%)
CTR
ZSTK
AS
CAL
AS+CAL
IPI
Sub G1
G0/G1
S
G2/M
B
APOPTOTIC CELLS (%)
KOPN8
NALM6
REH
C
PI
Annexin V-FITC
D
CTR ZSTK AS CAL AS+CAL IPI
PARP
Cleaved Caspase3
Actin
E
CELLS (%)

Figure 2

A

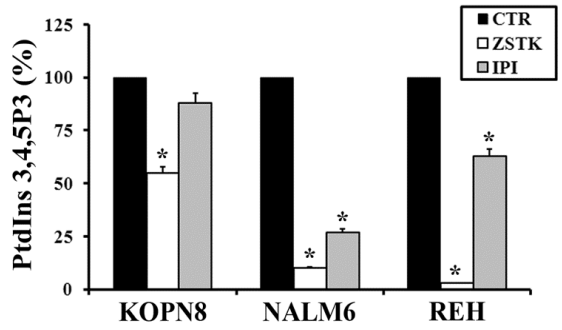
CTR
ZSTK
IPI
PtdIns 3,4,5P3 (%)
125
100
75
50
25
0
KOPN8
NALM6
REH

B

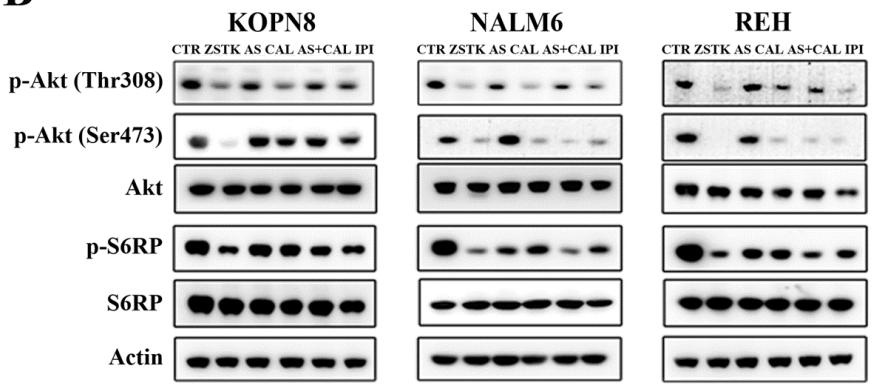
KOPN8
NALM6
REH
CTR ZSTK AS CAL AS+CAL IPI
CTR ZSTK AS CAL AS+CAL IPI
CTR ZSTK AS CAL AS+CAL IPI
p-Akt (Thr308)
p-Akt (Ser473)
Akt
p-S6RP
S6RP
Actin

Figure 3

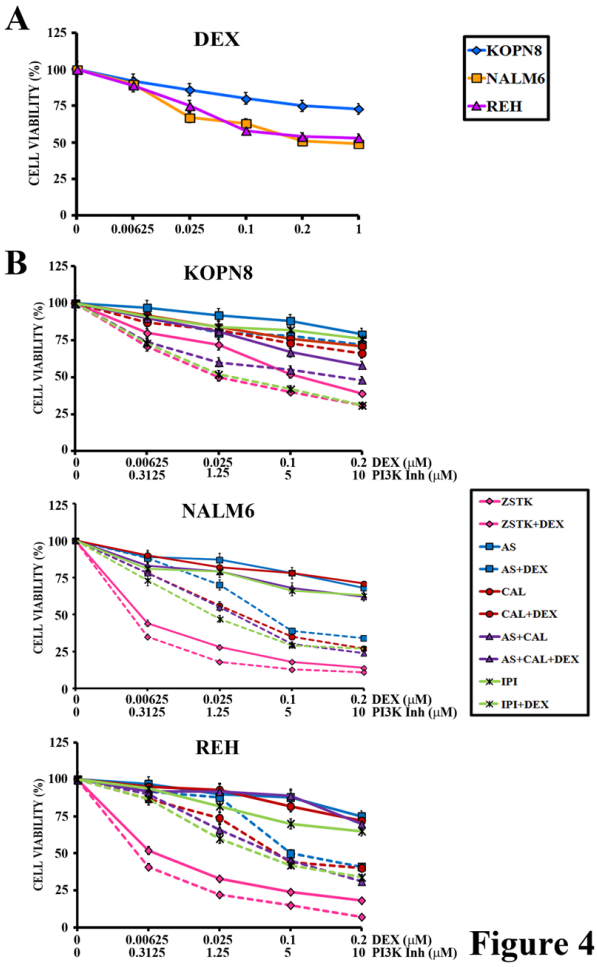
A
DEX
CELL VIABILITY (%)
125
100
75
50
25
0
0
0.00625
0.025
0.1
0.2
1
KOPN8
NALM6
REH
B
KOPN8
NALM6
REH
CELL VIABILITY (%)
0
0.00625
0.025
0.1
0.2 DEX (μM)
0
0.3125
1.25
5
10 PI3K Inh (μM)
ZSTK
ZSTK+DEX
AS
AS+DEX
CAL
CAL+DEX
AS+CAL
AS+CAL+DEX
IPI
IPI+DEX

Figure 4

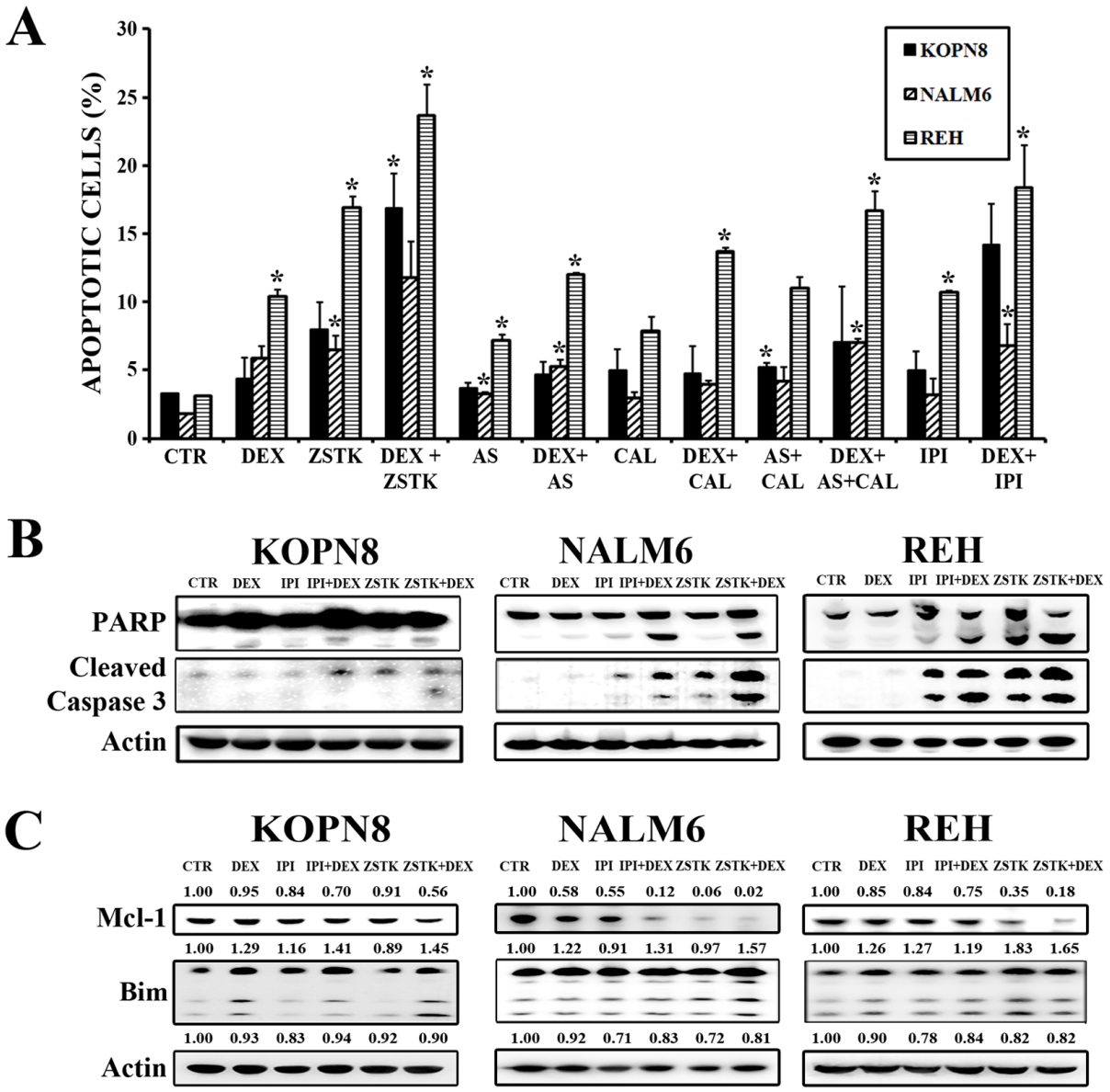
A
APOPTOTIC CELLS (%)
KOPN8
NALM6
REH
CTR
DEX
ZSTK
DEX + ZSTK
AS
DEX+ AS
CAL
DEX+ CAL
AS+ CAL
DEX+ AS+CAL
IPI
DEX+ IPI
B
KOPN8
NALM6
REH
CTR DEX IPI IPI+DEX ZSTK ZSTK+DEX
PARP
Cleaved Caspase 3
Actin
C
KOPN8
NALM6
REH
CTR DEX IPI IPI+DEX ZSTK ZSTK+DEX
1.00 0.95 0.84 0.70 0.91 0.56
1.00 0.58 0.55 0.12 0.06 0.02
1.00 0.85 0.84 0.75 0.35 0.18
Mcl-1
1.00 1.29 1.16 1.41 0.89 1.45
1.00 1.22 0.91 1.31 0.97 1.57
1.00 1.26 1.27 1.19 1.83 1.65
Bim
1.00 0.93 0.83 0.94 0.92 0.90
1.00 0.92 0.71 0.83 0.72 0.81
1.00 0.90 0.78 0.84 0.82 0.82
Actin

Figure 5

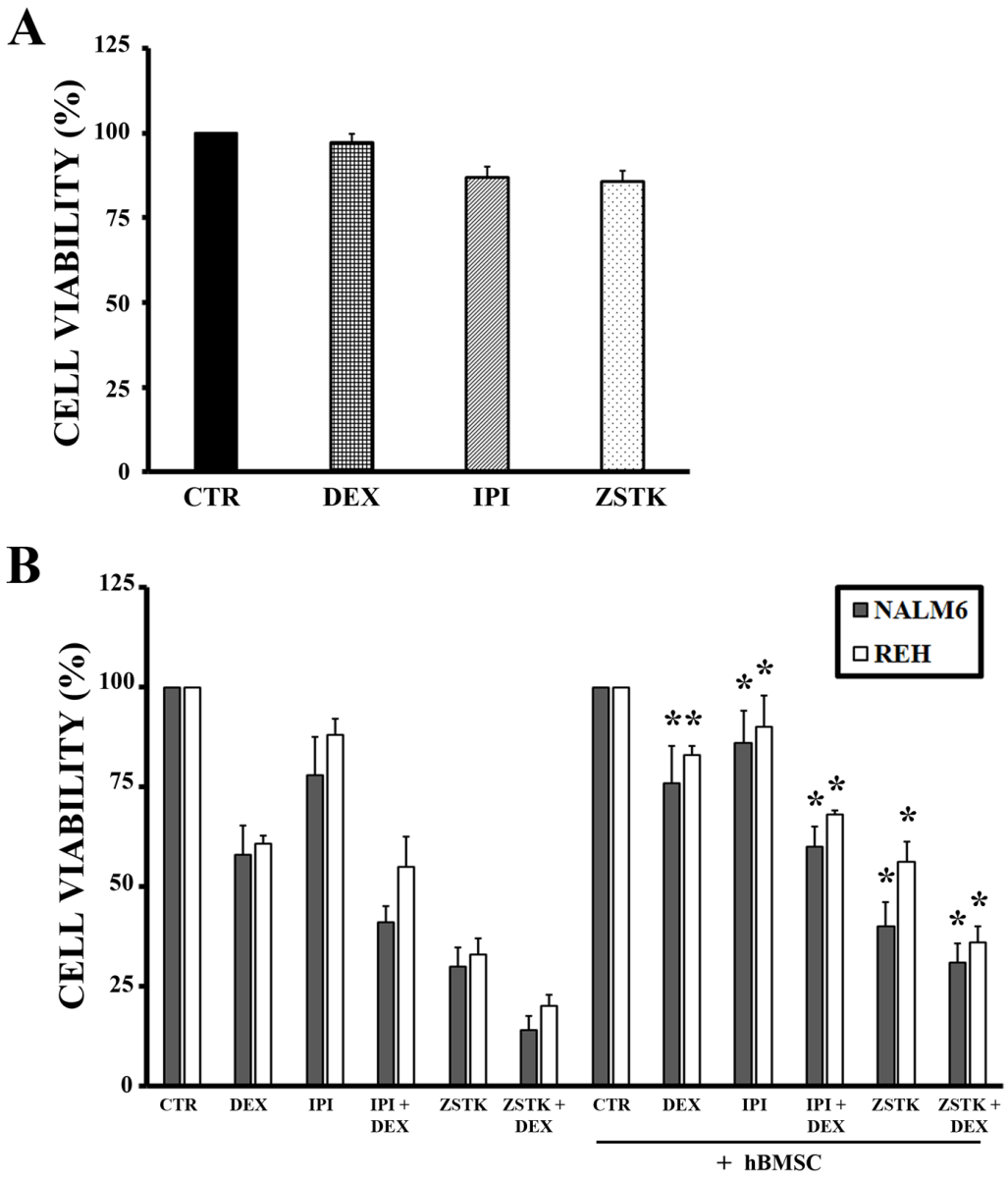
A
CELL VIABILITY (%)
125
100
75
50
25
0
CTR
DEX
IPI
ZSTK
B
CELL VIABILITY (%)
NALM6
REH
CTR
DEX
IPI
IPI + DEX
ZSTK
ZSTK + DEX
+ hBMSC

Figure 6

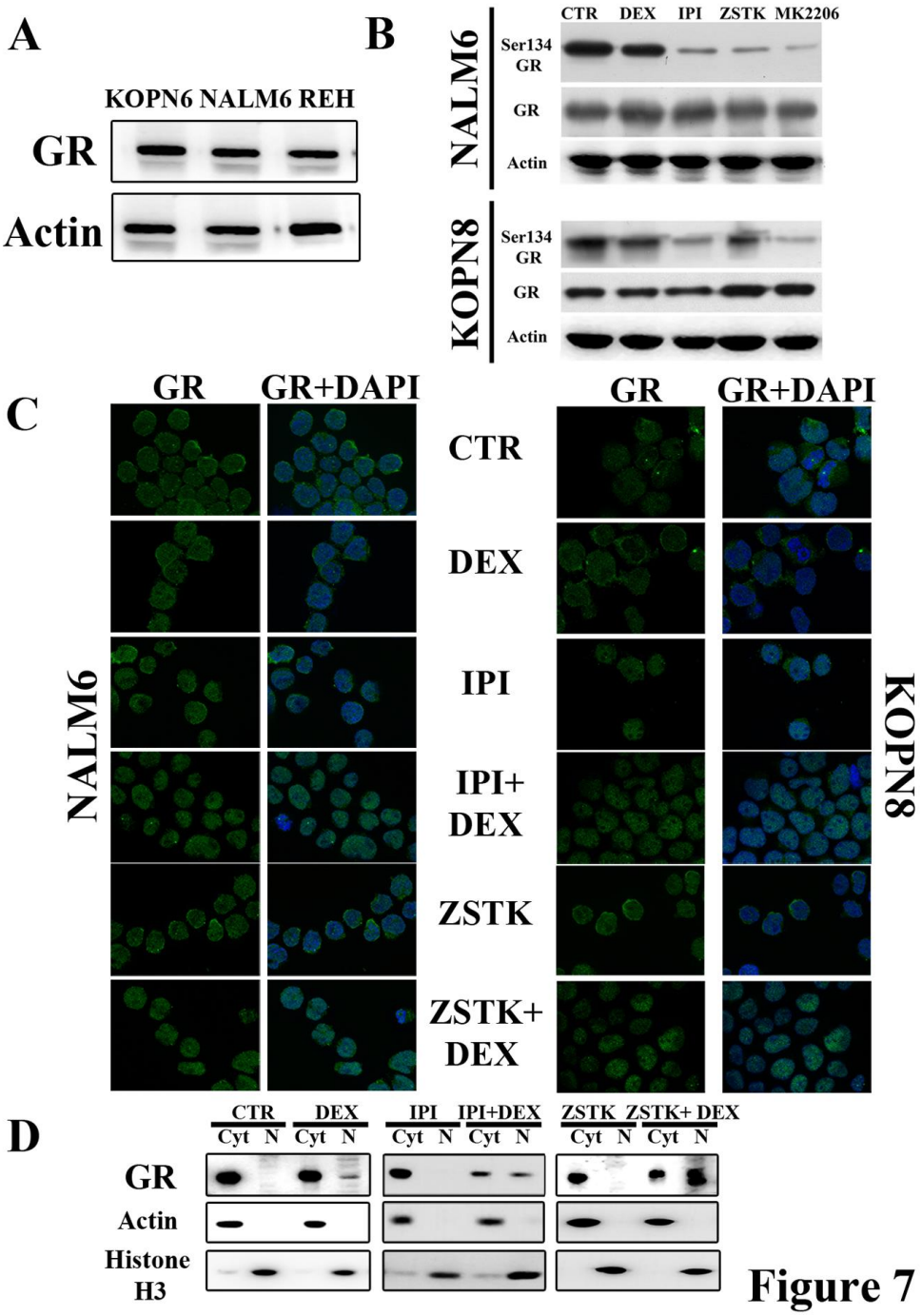
A
KOPN6 NALM6 REH
GR
Actin
B
CTR DEX IPI ZSTK MK2206
NALM6
Ser134 GR
GR
Actin
KOPN8
Ser134 GR
GR
Actin
C
GR
GR+DAPI
GR
GR+DAPI
NALM6
KOPN8
CTR
DEX
IPI
IPI+ DEX
ZSTK
ZSTK+ DEX
D
CTR DEX IPI IPI+DEX ZSTK ZSTK+ DEX
Cyt N Cyt N Cyt N Cyt N Cyt N Cyt N
GR
Actin
Histone H3

Figure 7

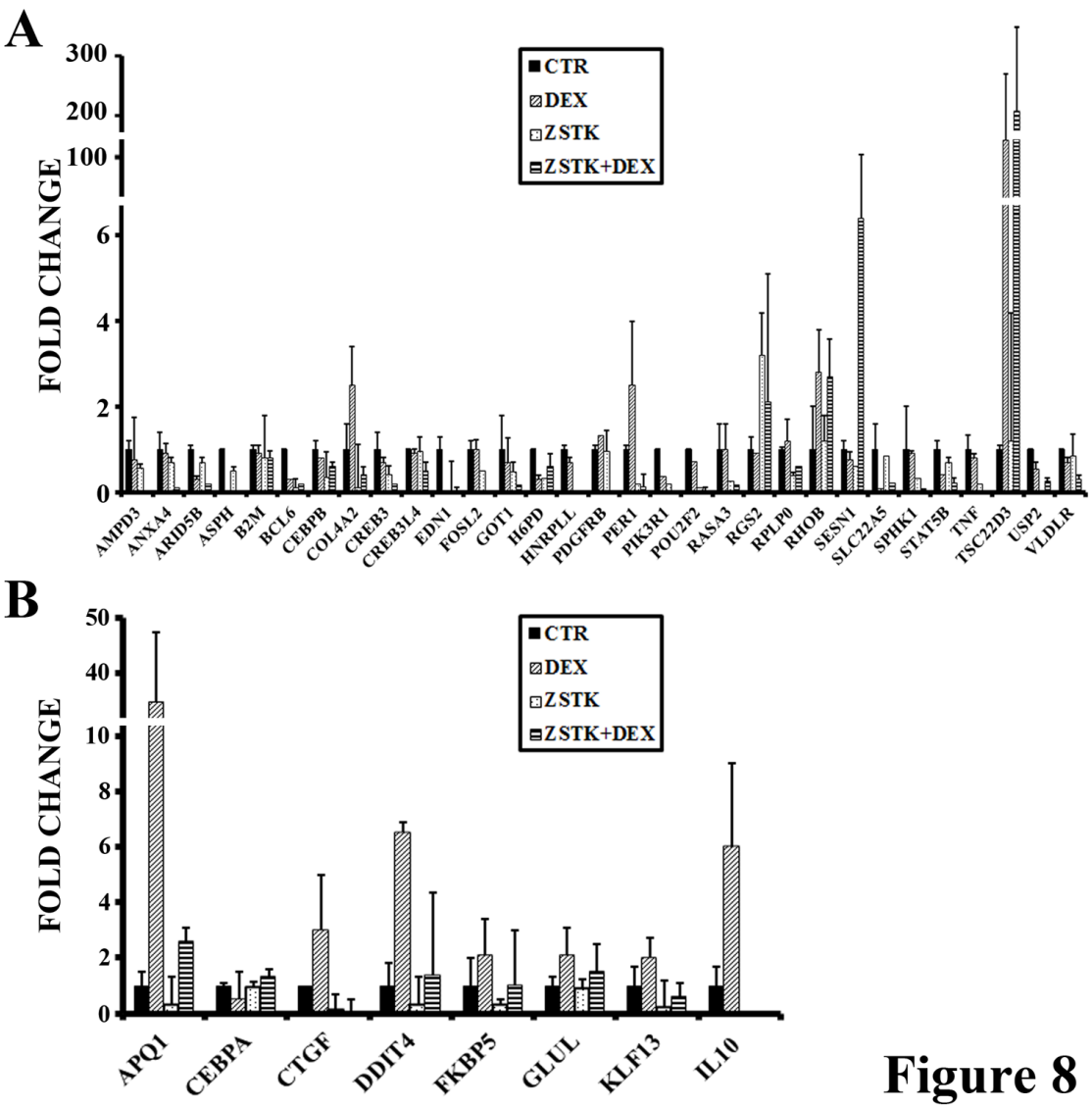
A
FOLD CHANGE
300
200
100
6
4
2
0
CTR
DEX
ZSTK
ZSTK+DEX
AMPD3
ANXA4
ARID5B
ASPH
B2M
BCL6
CEBPB
COL4A2
CREB3
CREB3L4
EDN1
FOSL2
GOT1
H6PD
HNRPLL
PDGFRB
PER1
PIK3R1
POU2F2
RASA3
RGS2
RPLP0
RHOB
SESN1
SLC22A5
SPHK1
STAT5B
TNF
TSC22D3
USP2
VLDLR
B
FOLD CHANGE
50
40
10
8
6
4
2
0
CTR
DEX
ZSTK
ZSTK+DEX
APQ1
CEBPA
CTGF
DDIT4
FKBP5
GLUL
KLF13
IL10

Figure 8

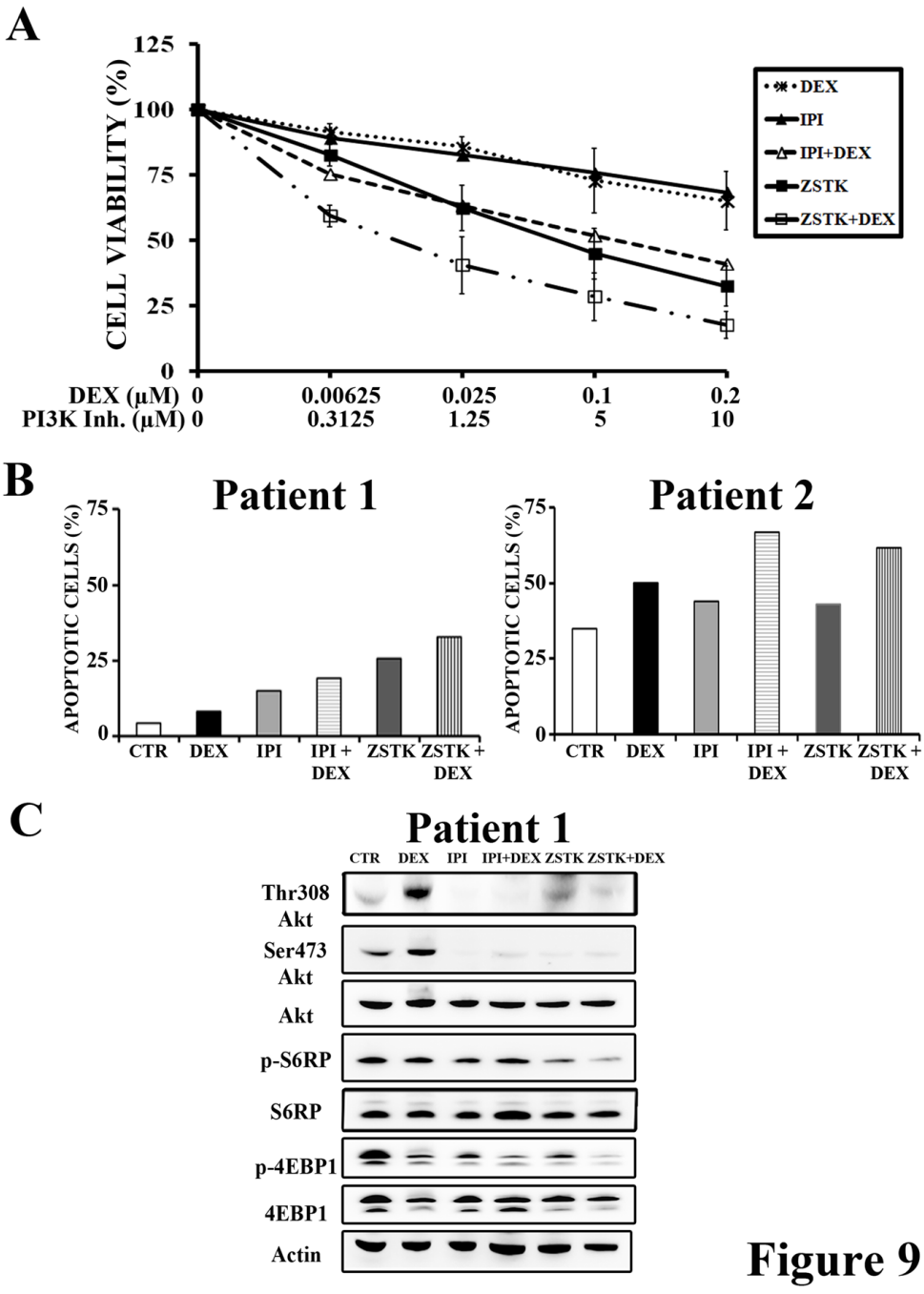
A
CELL VIABILITY (%)
125
100
75
50
25
0
DEX
IPI
IPI+DEX
ZSTK
ZSTK+DEX
DEX (μM) 0 0.00625 0.025 0.1 0.2
PI3K Inh. (μM) 0 0.3125 1.25 5 10
B
Patient 1
Patient 2
APOPTOTIC CELLS (%)
75
50
25
0
CTR
DEX
IPI
IPI + DEX
ZSTK
ZSTK + DEX
C
Patient 1
CTR DEX IPI IPI+DEX ZSTK ZSTK+DEX
Thr308 Akt
Ser473 Akt
Akt
p-S6RP
S6RP
p-4EBP1
4EBP1
Actin

Figure 9